DESIGN AND CONSTRUCT DISCRETE COMPOUND PARABOLIC CONCENTRATOR INTEGRATED COLLECTOR STORAGE SOLAR WATER HEATER (CPC ICSSWH)

KHONG DEWITT

A project report submitted in partial fulfilment of the requirements for the award of the degree of Bachelor of Engineering (Hons) Industrial Engineering

Faculty of Engineering and Green Technology
Universiti Tunku Abdul Rahman

January 2018

DECLARATION

I hereby declare that this project report is based on my original work except for citations and quotations which have been duly acknowledged. I also declare that it has not been previously and concurrently submitted for any other degree or award at UTAR or other institutions.

Signature : ___________________________

Name : KHONG DEWITT

ID No. : 13AGB03534

Date : ___________________________

APPROVAL FOR SUBMISSION

I certify that this project report entitled **“DESIGN AND CONSTRUCT DISCRETE COMPOUND PARABOLIC CONCENTRATOR INTEGRATED COLLECTOR STORAGE SOLAR WATER HEATER (CPC ICSSWH)”** was prepared by **KHONG DEWITT** has met the required standard for submission in partial fulfilment of the requirements for the award of Bachelor of Engineering (Hons) Industrial Engineering at Universiti Tunku Abdul Rahman.

Approved by,

Signature : _________________________

Supervisor : Dr. Tan Ming Hui

Date : _________________________

Specially dedicated to

my beloved family

ACKNOWLEDGEMENTS

I would like to thank everyone who had contributed to the successful completion of this project. I would like to express my gratitude to my research supervisor, Dr. Tan Ming Hui for his invaluable advice, guidance and his enormous patience throughout the development of the research.

In addition, I would also like to express my gratitude to my loving parent and friends who had helped and given me encouragement throughout this project.

Furthermore, I would like to express my gratitude to Mr. Mohd. Syahrul Husni bin Hassan, Mr. Khairul Hafiz bin Mohamad and Mr. Thong Marn Foo for their assistance throughout this project.

DESIGN AND CONSTRUCT DISCRETE COMPOUND PARABOLIC CONCENTRATOR INTEGRATED COLLECTOR STORAGE SOLAR WATER HEATER (CPC ICSSWH)

ABSTRACT

Solar energy is clean, free and sustainable compared to fossil fuels. One of the typical utilization of solar energy is solar water heating system where it is a well-developed application for water heating. There are numerous types of solar water heater (SWH) systems existed in the market to suit customers' various demands. For instance, flat plate collector SWH, evacuated tube collector SWH, parabolic trough collector SWH and integrated collector storage SWH. This study presents a discrete compound parabolic concentrator integrated collector storage solar water heater (CPC ICSSWH) that is easy to be fabricated and it is a passive system in which active pump and sun tracking is not required. The discrete compound parabolic concentrator (CPC) was constructed by several rectangular facet mirrors and a wide acceptance angle of 56° was used so that sun tracking can be eliminated, thus making it very suitable for domestic purposes. Ray tracing simulation, system performance analysis and the cost analysis of the discrete CPC ICSSWH were carried out and presented in details. The discrete CPC ICSSWH can achieve a theoretical maximum system efficiency of 63.39% and has attained highest water temperature of 70.6°C with total payback period of 6.25 years.

TABLE OF CONTENTS

LIST OF TABLES

LIST OF FIGURES

LIST OF SYMBOLS / ABBREVIATIONS

A_{a}	aperture area of concentrating solar collector, m^2
A_{ap}	area of the entry aperture of discrete CPC, m^2
A_{c}	area of flat plate collector, m^2
A_{r}	absorber area of concentrating solar collector, m^2
a	half entry aperture of CPC, cm
a'	half exit aperture of CPC, cm
CR	geometric concentration ratio
CR_o	optical concentration ratio
c_{water}	specific heat capacity of water, J/(kg·°C)
$\mathrm{d}e_{\mathrm{c}}/\mathrm{d}t$	rate of internal energy storage in the collector, J/s
g	gravitational acceleration, m/s^{-2}
H	height of the legs, m
H_{cpc}	height of the CPC, cm
I_{a}	aperture's solar flux, W/m^2
I_{ave}	average global solar irradiance, W/m^2
I_{c}	solar irradiation on a collector surface, W/m^2
I_{r}	receiver's solar flux, W/m^2
i	interest rate, %
j	inflation rate of the fuel, %
L	height of the collector, m
m	mass of water, kg
n	day number during a year
n_{mirror}	number of mirror
n_{pay}	payback period, year
P_{ann}	annual saved fuel cost, RM/year
ΔP_{FLOW}	change in the fluid loop's flow pressure, $kg/(m \cdot s^2)$

$\Delta P_{\mathrm{BUOYANT}}$	pressure change of the buoyant force, kg/(m·s^2)
Q_{col}	collected thermal energy, J
$Q_{incident}$	total amount of incident solar energy radiated on the discrete CPC ICSSWH entry aperture area, J
q_{u}	rate of heat transfer from the collector–absorber plate to the working fluid, J/s
q_{loss}	rate of heat transfer (or heat loss) from the collector–absorber plate to the surroundings, J/s
S_{total}	total retail cost of the discrete CPC ICSSWH, RM
$T_{ave,\ ambient}$	average ambient temperature over an interval time, °C
$T_{ave,\ heating}$	average water temperature in the storage tank over the period of heating for an interval time, °C
$T_{i,amb}$	initial ambient temperature over the interval of time, °C
$T_{i,\ heating}$	initial heating temperature of the water, °C
$T_{f,amb}$	final ambient temperature over the interval of time, °C
$T_{f,\ heating}$	final heating temperature of the water, °C
Δt	time interval, s
x	x-coordinate of the point
Δx	difference in x-coordinates between the top edge and bottom edge of the mirror
y	y-coordinate of the point
Δy	difference in y-coordinates between the top edge and bottom edge of the mirror
α_{s}	collector–absorber plate surface’s solar absorptance
β	tilt angle, °
δ_{s}	solar declination, °
η_c	instantaneous efficiency of a collector
η_{sys}	system efficiency
ρ_{out}	collector outlet fluid density, kg/m^3
ρ_{stor}	tank fluid density, kg/m^3
$\rho(x)$	local collector fluid density, kg/m^3
τ_{s}	collector cover(s)’ effective solar transmittance

θ_a	half acceptance angle, °
θ_i	first slope angle, °
θ_f	final slope angle, °
$\Delta\theta_m$	delta angle allocated for each mirror, °
$\Delta\theta_o$	overall delta angle, °

CAD	computer aided design
CPC	compound parabolic concentrator
GHI	global horizontal irradiance, W/m^2
GUI	graphic user interface
ICSSWH	integrated collector storage solar water heater
IGES	initial graphics exchange specification
IPH	industrial process heat
L	latitude

LIST OF APPENDICES

CHAPTER 1

INTRODUCTION

1.1 Overview

Solar energy is the Earth's prime energy source which is clean, free and sustainable. The Sun delivers ample solar energy to power the living creatures on Earth and warm up the Earth (Ramlow and Nusz, 2010). The application of solar technologies is vital for both developing and developed countries. The reasons are solar energy can be obtained infinitely and practically zero fuel cost incurred to the people. Additionally, the dependence on the fossil fuel energy can be then minimised or eradicated completely. By reducing the usage of fossil fuel energy, the people can enjoy the advantages of having cleaner environment and better health. For example, the pollution of the air, water, and land can be reduced with the installation of solar technologies (Makofske, 2015).

In the renewable energy sector, the progression of solar water heater is considered as one of the fastest among other technologies (Kumar and Rosen, 2011). The continuous development of the research enables the solar water heating to have higher sustainability, higher efficiency and more cost effective (Devanarayanan and Murugavel, 2014). There are two general types of the designs of solar water heater, they are natural convection (passive) and forced circulation (active). Typical collectors used in the solar water heater system are flat-plate, evacuated-tube, and concentrator collector.

Sabiha et al. (2015) stated that the flat plate collector is famous for its simplicity in design and minimal cost of maintenance. However, the disadvantages of flat plate collectors are that solar tracking is absent and the glass cover is subjected to heat convective loss. Hence, evacuated tube solar collector is innovated whereby its efficiency is greater than flat plate collector because vacuum is present in the design. Nevertheless, evacuated tube collector has its drawbacks. Since the evacuated tubes are made of annealed glass, they are very fragile and must be handled with care. The initial cost is also high for the construction of evacuated tube collector. Since both the flat plate collector and evacuated tube collector is non-concentrating, a concentrating collector is recommended in solar water heater system to further enhance the thermal performance.

One of the concentrating collectors is parabolic trough collector. Singh, Singh and Yadav (2012) had designed and constructed a parabolic trough solar water heater for analysis. The system requires to track the sun manually. Based on their studies, they were able to obtain the maximum water temperature of 69℃ and an efficiency of 18.23% when aluminium tube without glass cover was used; maximum water temperature of 75℃ and efficiency of 20.25% when copper tube without glass cover was used. Another concentrating collector is compound parabolic concentrator (CPC). According to Singh, Lazarus and Souliotis (2016), compound parabolic concentrator collector allows all the incident rays to be reflected on the absorber. Tracking of the sun is not necessary.

The integrated collector storage solar water heater (ICSSWH) systems are famous for its simplicity in its operating function and design. The ICSSWH systems are less costly compared to other solar water heater designs. The uniqueness of the ICSSWH systems lie on the combination of hot water storage tank and the solar energy absorber. With that said, the ICSSWH systems are built as a single unit. Furthermore, ICSSWH is passive system, hence no active pump is required and cost incurred on purchasing the pump can be eliminated. The benefits of ICSSWH systems are it is anti-freezing because of its huge thermal mass correlated with type of absorber surface used, great reliability as it can provide hot water for many years, and little maintenance is needed periodically (Kumar and Rosen, 2010).

The problems of ICSSWH systems are that they are subjected to suffer from the ambient heat losses greatly. The heat losses are especially obvious during non-collection periods and night time. Hence, the study on the improvement of the ICSSWH systems’ thermal performance is carried out to further enhance the system especially for overnight applications. The concentration ratio, CR of more than 1 can be attained when the compound parabolic concentrators (CPC) are integrated into the ICSSWH system. Therefore, water storage thermal losses can be lessened because the absorber area is smaller than the aperture surface area (Souliotis et al., 2012). Furthermore, Kumar and Rosen (2011) further mentioned some other cases of enhancement applied on the ICSSWH systems are transparent insulation, night insulation cover, and multiple glazing layers. The authors stated that the installation of single glazing and night insulation cover as well as the installation of double glazing without night insulation cover to the ICSSWH have higher thermal outputs compared to other similar systems mounted with single glass cover, transparent insulation and baffle plate.

1.2 Problem Statements

Based on the researches done by Kumar and Rosen (2010); Souliotis et al. (2012), the researchers focus on improving the ICSSWH systems by adding features such as glazing to reduce the heat losses. Flat plate and evacuated tube collectors are non-concentrating. Concentrating collector is recommended to be incorporated into the ICSSWH system. However, not all concentrating solar collectors are suitable. Parabolic trough collector is not recommended because it requires solar tracking. Therefore, compound parabolic concentrator (CPC) is preferred to be built into the ICSSWH system in order to attain concentration ratio of more than 1 and without sun tracking. However, the underlying problems when constructing CPC reflectors is that CPC is considered to have high geometry complexity due to its curvature. They are very hard to be manufactured and therefore, specialised machines are required to manufacture such sophisticated design. Furthermore, there is high possibility that the manufacturing of CPC reflectors will have imperfection in terms of its symmetrical design.

Hence, the discovery of replacing the CPC profile with a much simpler design is required. Currently, there is no research on such matter. The new discrete optical geometry is based on the CPC geometry. However, the optical geometry of the new design will be completely different. With that said, the concentration ratio of the new collector geometry will also require further study. Lastly, the performance of the discrete CPC ICSSWH system needs to be evaluated.

1.3 Aims and Objectives

The objectives of the thesis are shown as following:

i) To design the optical geometry of the discrete CPC Integrated Collector Storage Solar Water Heater.

ii) To construct the discrete CPC Integrated Collector Storage Solar Water Heater.

iii) To evaluate the performance of the discrete CPC Integrated Collector Storage Solar Water Heater.

CHAPTER 2

LITERATURE REVIEW

2.1 Sun-Earth Geometrical Relationship

There is variation between the distance of the Sun and the Earth all year long. On June 21st, it is the summer solstice and the distance between the Sun and the earth is at maximum with a value of 1.521×10^{11} m. Meanwhile, the minimum distance between them is 1.471×10^{11} m and it occurs on December 21st, which is the winter solstice. Hence, the average of the distance between the Sun and the Earth is 1.496×10^{11} m throughout the year. Furthermore, the amount of solar radiation that is received by the Earth will be minimum on the summer solstice and maximum on the winter solstice (Goswami, 2015). Figure 2.1 illustrates the motion of the Earth around the Sun and their distance at a particular day.

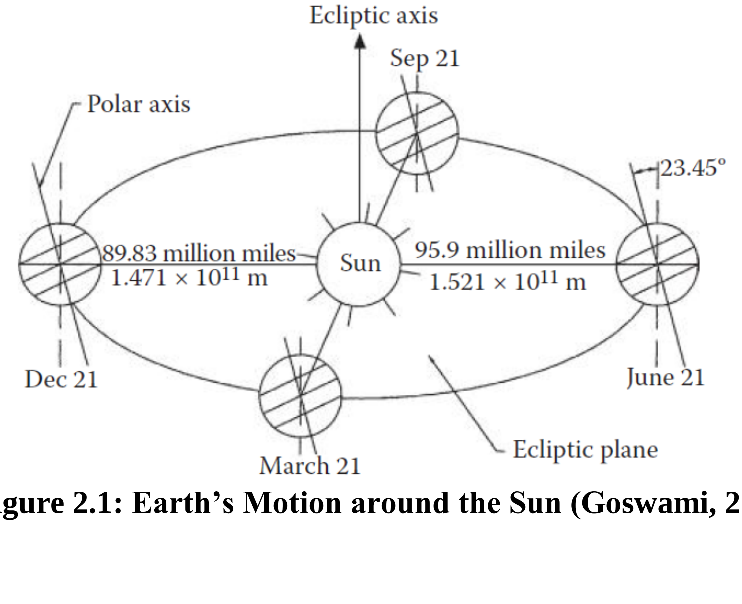

Figure 2.1: Earth's Motion around the Sun (Goswami, 2015)

According to Goswami (2015), the angle between the axis of self-rotation of the Earth to the Earth's ecliptic orbital plane around the Sun is 23.45˚. It is known as the solar declination, δ_s. Therefore, different locations on the Earth will experience changes in the seasons due to the tilt angle. The deviation of the declination angle is between -23.45° to +23.45° on December 21st and June 21st respectively. Besides, it can be deduced that the declination angle will have the exact value as the latitude of the Earth numerically whereby at noon of a particular day, the Sun will be directly above the head. For example, the tropics of Cancer and Capricorn have the latitudes of 23.45°N and 23.45°S respectively, as shown in Figure 2.2. On the other hand, there are some locations where the Sun will not rise exactly above the horizon plane. The Arctic and Antarctic circles are the location examples and they are positioned at the latitudes of 66 1/2°N and 66 1/2°S correspondingly. The value of the angle declination is denoted as positive for the north of the equator; negative at the south of the equator. The estimation of the solar declination can be calculated as following equation,

$$\delta_s = 23.45° \sin[360(284 + n)/365°] \tag{2.1}$$

where n is the day number during a year with January 1 being n = 1. However, the solar declination may be measured as a constant during any given day for most of the calculations.

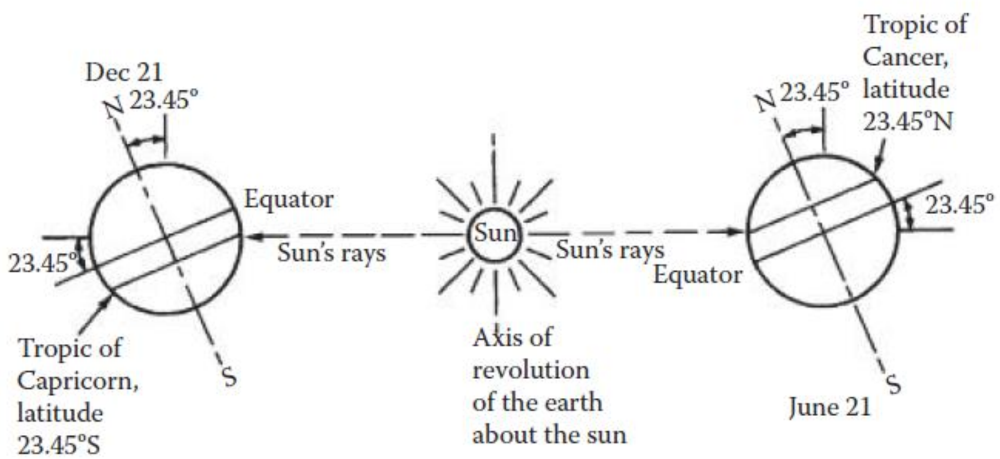

Figure 2.2: Tropics of Cancer and Capricorn Locations (Goswami, 2015)

2.2 Solar Water Heating Systems

Nowadays, one of the typical utilisation of solar energy is the solar water heating systems. They are being implemented for both domestic hot water applications and industrial process heat (IPH) applications depending on their system size (Goswami, 2015). Generally, there are two types of solar water heating systems, they are direct and indirect systems. Direct solar water heating system is open-loop, whereby the water used daily is heated by passing through the solar collector. Meanwhile, indirect solar water heating system is closed-loop. Solar fluid, a type of fluid for heat transfer, is prior heated in the collectors. The heat absorbed by the solar fluid is then transmitted to the domestic water in heat exchanger (Ramlow and Nusz, 2010).

The solar water heating systems can also be classified into forced circulation and natural circulation. For forced circulation, also known as active solar system, the solar-heated fluid is transported for direct usage or storage with the assistance of powered pumps. For example, cold regions greatly apply forced circulation water heaters; IPH applications; and commercialisation. For natural circulation, also known as passive solar system, it does not require much machine-driven system such as pumping, to function properly. Inexpensive and design simplicity are features of natural circulation solar water heaters (Goswami, 2015; Twidell and Weir, 2015).

Furthermore, the solar collector is another major concern during the construction of solar heating system. The collector functions as a tool to absorb the solar radiation and channel the energy received to the stored fluid (Twidell and Weir, 2015). There are a few types of solar collectors; for instance, Flat-Plate Collectors, Evacuated-Tube Collectors and Compound Parabolic Concentrator. The mentioned solar collectors have different thermal performances and concentration ratios respectively (Goswami, 2015).

There are numerous benefits for using solar water heating. The solar thermal panels require minimal space for installation. About two or three panels with an area of $2m^2$ respectively is needed for water heating. Next, they are inexpensive since less number of panels and space are needed for installation. Furthermore, it helps in reducing financial expense. This is because fuel and electricity are saved and only solar energy is utilised. The system is also considered to have good efficiency of about 80%. Lastly, carbon footprint is decreased. As solar energy is renewable, this indicates that no carbon dioxide is emitted (Morley, 2017).

Morley (2017) listed out some drawbacks of solar water heating. Maintenance on solar water heating system is suggested to be carried out yearly. As some of the designs may consist of parts such as mechanical pump, inspection is preferable to safeguard its optimal performance. In addition, a storage tank or cylinder is used to store water. Hence, extra area is required to accommodate the solar storage tank.

2.2.1 Natural Circulation Systems

In a solar water heater system, the concept of higher density fluid tends to flow below a lower density fluid to induce fluid movement through a collector can be incorporated (Close, 1962; Goswami, 2015). When heat from the sun approaches the liquid within the collector, the liquid is warmed up and creates a density difference. A natural circulation loop is established when the heated water flows up to the storage tank from the collector, whereas the water with lower temperature moves to the collector’s bottom from the storage tank. Thermosiphon loop is another reference to this natural circulation loop (Figure 2.3). This water heater is considered as passive because of the absence of mechanical pump. The storage tank must be placed at a position higher than the collector in order for the system to be functional (Goswami, 2015).

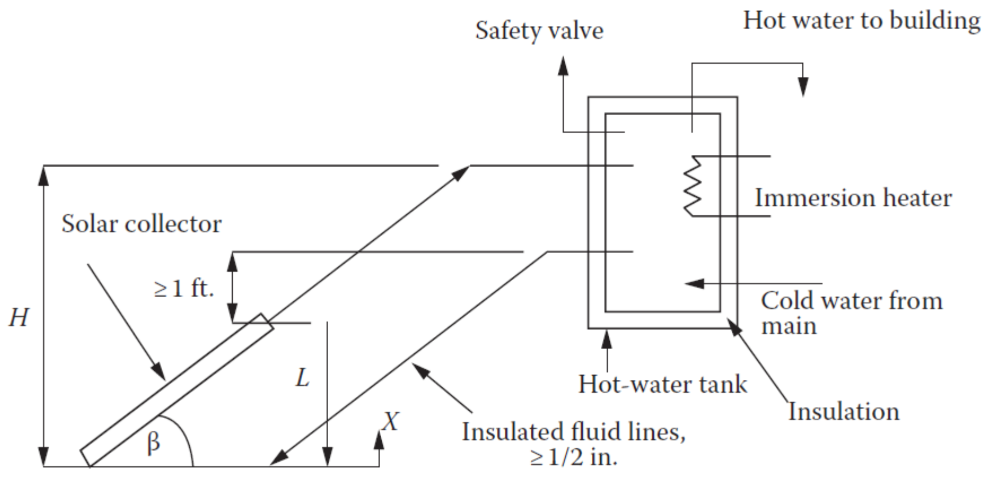

Figure 2.3: Thermosiphon Loop Applied in the Natural Circulation (Goswami, 2015)

According to Goswami (2015), the drop in the fluid loop's flow pressure and the pressure change of the buoyant force due to the densities change in the fluid's hot and cold legs must be equivalent:

$$\Delta P_{\mathrm{FLOW}} = \Delta P_{\mathrm{BUOYANT}} \tag{2.2}$$
$$= \rho_{\mathrm{stor}} gH - \int \rho(x) g\,\mathrm{d}x + \rho_{\mathrm{out}} g(H - L)$$

where H is height of the legs, m; L is the height of the collector, m; $\rho(x)$ is the local collector fluid density, kg/m^3; ρ_{stor} is the tank fluid density, kg/m^3; ρ_{out} is the collector outlet fluid density, kg/m^3; g is the gravitational acceleration, m/s^{-2}, note that the latter two densities were assumed to be uniform.

Furthermore, the tilt angle, β must be same with the value of latitude, L. This is due to the small variation in the loads of the hot water system annually. Plus, during the middle of a sunny day, the obtained temperature gap between the collector's inlet and outlet water is around 8˚C to 11˚C typically. Other than that, the absorber's top header should be located below the storage tank's cold fitting legs with a minimum distance of 30cm. This is to ensure that the water does not reverse its flow and results in heat loss to the environment (Close, 1962; Goswami, 2015).

Furthermore, an electrical immersion heater is recommended to be installed to the solar water heater system. It can act as heat provider in case of prolonged rainy and cloudy seasons. In order to boost stratification, the immersion heater should be positioned close to the upper of the tank. With that, the heated water is able to achieve the necessary temperature. Water flow rate can be maintained at high velocity through tank stratification. In addition, heat loss can be minimized by applying insulation over the whole tank surface (Goswami, 2015).

Lastly, thermosiphon design has its limitation. A nonfreezing fluid is required to ensure the system operates normally in cold climates. A heat exchanger must be installed between the moveable water storage tank and solar collector. For example, immersion-coil type or shell-and-tube type heat exchangers can be utilized; however, operation with high efficiency necessitates higher flow rates in which thermosiphon failed to provide. The heat exchanger coil welded to the outer tank surface may functions properly in mild freezing climates provided antifreeze is applied together with it. Hence, the thermosiphon works best at nonfreezing climates (Goswami, 2015).

2.2.2 Forced Circulation Systems

In freezing climate, a water pump is needed because of the storage tank is built underneath the solar collector or inside the building. Anti-freezing fluid is allowed since that the fluid circuit through the collector is disjointed. A water storage tank of 100 to 300 liters is sufficient to store one day’s hot water supply for domestic uses. Hence, a small mechanical pump is enough to power the system. Figure 2.4 illustrates the solar water heater system with forced convection. Each time the fluid passes through the collector, the water temperature increment is 5˚C to 10˚C approximately. However, the difference between inlet and outlet temperature of the collector and solar irradiance, G are the factors affecting the temperature increment (Twidell and Weir, 2015).

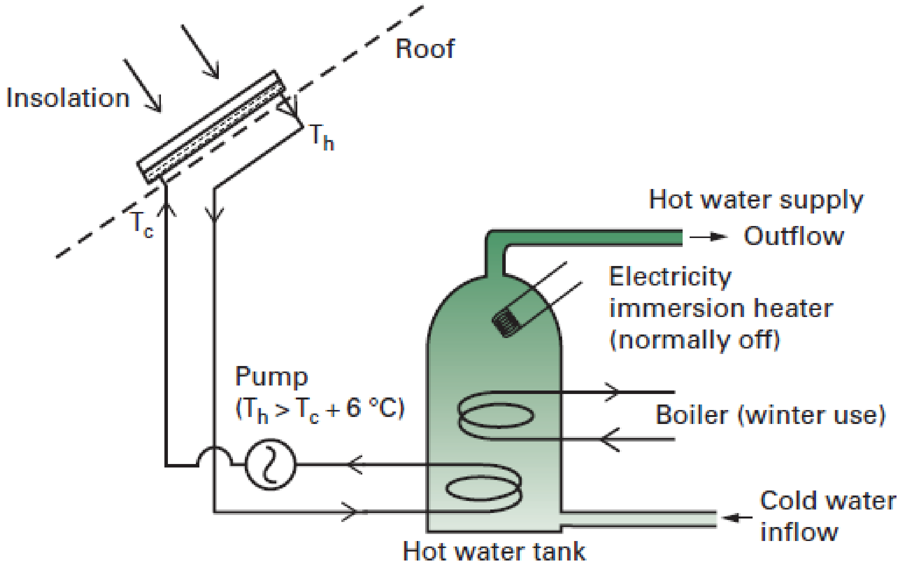

Figure 2.4: Solar Water Heater with Forced Circulation (Twidell and Weir, 2015)

A controlled variable-speed pump is needed for optimal performance. In reality, a constant-speed pump is introduced in the forced circulation system mainly because it is inexpensive. Main electricity or a small photovoltaic panel are examples of the source power for the mechanical pump. The collector output temperature is controlled to have roughly 5˚C higher than the input temperature by switching on and off the pump automatically. The advantages of automatic switch are to prolong the lifespan of the pump from unnecessary usage and to reduce heat loss from the collector at night and as well as during low sunlight day. Moreover, in order to avoid boiling issue, a temperature sensor is installed inside the top of the tank for monitoring purpose (Twidell and Weir, 2015).

Next, the tank and its heat transfer devices must be taken into consideration in the overall design of the solar water heater with high effectiveness. Some other methods to achieve the goal are to add insulation since it is not costly; and the hot pipes' length reduction by adjusting the tank position. The hottest water must always be retained at the upper tank with stable stratification and the water input must be from the coldest and lowest depth of the tank in the design. However, the difficulty level to attain these two conditions is very high. This is due to the possible pollution or freezing incurred to the water if it is to flow through the collector. Plus, the height of the tank where tapping of water occur is also another factor for the obtained temperature of the water (Twidell and Weir, 2015).

2.2.3 Integrated Collector Storage System

Devanarayanan and Murugavel (2014) stated that integrated collector storage solar water heater (ICSSWH) is consisted of water storage tank and the solar collector. They are joint to become a single unit. Compared to the thermosiphon solar water heater with flat plate collectors or evacuated tubes, ICSSWH is better due to lower cost and uncomplicated construction. Singh, Lazarus and Souliotis (2016) also reviewed on the recent progress in ICS solar water heater. The authors stated that the conversion rate of solar radiation into heat is deemed considerable when the solar radiation is focused. The design and manufacture of ICS systems are very sensible as they are visually attractive and compact. Furthermore, they claimed that ICS systems have high collection efficiency factor. Devanarayan and Murugavel (2014) mentioned that the problem faced by the ICSSWH is that during night time, the heat loss is substantial. This is because the storage tank is also acts as the absorber tank, hence, thermal insulation cannot be applied since the absorber tank has to receive solar radiation. Utilisation of compound parabolic concentrator (CPC) collector is one of the approaches to boost the ICSSWH performance since it allows the collection and reflection of most of the solar rays on the absorber tank surface.

Kumar and Rosen (2010) modified the absorber surface to be corrugated to study the ICSSWH thermal performance. The authors deduced that the quantity of solar radiation received by the absorber and the transfer rate of heat energy between absorber surface and the water are the factors that affect the thermal performance. In the experiment, the minimum and maximum depths of corrugation are 0.0004 m and 0.001 m respectively. Assumption is made that during the collection of solar radiation, the corrugated surface is treated as plane surface since the corrugation depth is small which is less than 1 mm. Next, they corrugated the absorber surface to increase the surface area for solar radiation exposure. The characteristic length of the corrugated surface is also greater, thus allowing greater heat transfer convectively. Furthermore, 20 galvanised iron sheets are used to build the tank surfaces. The tank can accommodate 100 litres of water. Fibreglass with 5cm thickness is used to insulate the sides and bottom of the tank. The top surface of the tank is covered by a transparent glass cover to further reduce the heat loss. Based on the results, the maximum water temperature obtained increases from 53℃ to 64℃ when the deepness of corrugation is increased from 0.0004m to 0.001m. Nevertheless, the efficiency is reduced with the increase in corrugation depth. For the system with absence of cover for night insulation, the obtained efficiency is from 40% to 35%; when the night insulation cover is added to the system, the attained efficiency is from 46.8% to 42.4% with the increase depth of corrugation. The authors then reasoned that at higher temperature, the heat loss in the system is greater, therefore the efficiency is reduced. Hence, the system efficiency can be improved by ensuring the extraction of water is continuous.

Varghese, Samsher and Manjunath (2017) studied on the compound parabolic concentrator integrated collector storage solar water heater for domestic use. The acceptance angle used is 64° to ensure solar tracking is required occasionally. For the design of the system, the storage tank can keep 100 litres of water. It is painted black to increase the absorptivity. A wooden cradle is built to support the reflector. Phenol bonded plywood sheets are used to construct the wooden cradle. Meanwhile, stainless steel with thickness of 18 gauge is used to form the reflector. The reflector and the tank are then assembled into the wooden cradle. To further insulate the system thermally, 4mm clear float glass covers are used to minimise the heat loss. The inner gap between the reflector and the wooden cradle is filled with glass wool insulating material to ensure the heat loss is minimised. Air gap is also added to increase thermal insulation. The maximum temperature of the water and thermal efficiency is 53℃ and 38.1%. Without the air gap, the maximum temperature of water and thermal efficiency is 44℃ and 29.7%. Hence, air gap is one of the approaches to be used in the design to enhance the retention of heat.

2.3 Solar Collectors

A solar collector is a unique heat exchanger that converts the solar radiant energy to heat energy (Duffie and Beckham, 2013). The most common types of solar collectors are flat-plate collector, evacuated-tube collector, and concentrating solar collector.

2.3.1 Flat-Plate Collectors

Flat-Plate Collector is deemed as the noncomplex solar collector. It is broadly used in solar water heating systems fabrication for commercialisation. A simple flat-plate collector is comprised of a few components, namely glazing covers, absorber surface, medium for heat transfer, thermal insulator, and container (Figure 2.5). Glazing cover, also known as transparent cover, is utilised for minimisation of heat loss due to convection. It is also needed for shorter wavelength of solar radiation transmission; longer wavelength of solar secondary absorption of radiation is prohibited simultaneously. Typical example of glazing material is glass. Next, absorber is vital for incident solar radiation absorption to its greatest degree; improve the heat transfer efficiency to fluid; and minimise radiation reemission. Aluminium, copper, and stainless steel are some examples of materials used in making the absorber. In some cases, selective covering or black paint is applied on the absorber in order to enhance the effectiveness of solar radiation absorption (Goswami, 2015).

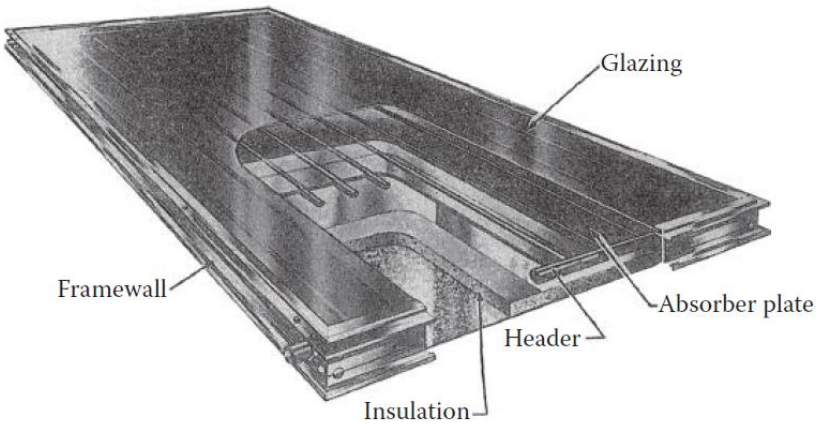

Figure 2.5: Flat-plate Collector (Goswami, 2015)

2.3.1.1 Energy Balance for a Flat-Plate Collector

Goswami (2015) stated that the percentage of the arriving radiation converted as valuable energy to the working fluid is analysed by appraising the energy balance. The absorber plate's energy balance formula for a flat plate collector of an area, A_c is

$$I_C A_C \tau_S \alpha_S = q_u + q_{loss} + \frac{de_c}{dt} \tag{2.3}$$

where I_c is the solar irradiation on a collector surface; τ_s is the collector cover(s)' effective solar transmittance; α_s is the collector–absorber plate surface's solar absorptance; q_u is rate of heat transfer from the collector–absorber plate to the working fluid; q_{loss} is rate of heat transfer (or heat loss) from the collector–absorber plate to the surroundings; de_c/dt is rate of internal energy storage in the collector.

Meanwhile, the instantaneous efficiency of a collector η_c can be calculated by obtaining the ratio of the useful energy conveyed to the total inbound solar energy,

$$\eta_c = \frac{q_u}{A_c I_c} \tag{2.4}$$

In reality, a finite time period is required to evaluate the efficiency. The design system performance must be studied for longer period, t to obtain the average efficiency

$$\eta_c = \frac{\int_0^1 q_u dt}{\int_0^1 A_c I_c dt} \tag{2.5}$$

Jayakanth et al. (2017) had studied the flat-plate collector and evacuated tubes on solar water heater. The authors claimed that this solar design has high efficiency and most cost-saving. On the design perspective, numerous materials are used in the making of the system as well as improve its thermal performance. Mild steel, copper tube, acrylic fibre, galvanised iron sheet, and high-density polyethylene pipe are needed to complete the system. Moreover, heat reduction is achieved by inserting the glass wool and sawdust between the inner and outer tank. The tilt angle is also adjusted to ensure highest solar radiation absorption. The system is active by using pump to make certain that water is flowed endlessly. For complete cycle, the difference in temperature increment of water with mass of 25kg is 16˚C from 34˚C to 50˚C after 100 minutes heating and the calculated collector efficiency is 18.19%. However, it is determined that the maximum efficiency can be attained if the (change in temperature / change in time) with respect to time is constant at its maximum value. From the experiment, 8˚C is increased within 15 minutes and the highest collector efficiency of 60% is obtained.

2.3.2 Evacuated-tube Collectors

Alghoul et al. (2005) stated that the evacuated-tube collector was an innovation in the design of solar collectors. This is because of its breakthrough on applying benefit of vacuum insulation into the design. The evacuated-tube collector has greater efficiency than flat-plate collectors at higher temperature. The main purpose of this collector is to fully avoid the loss of absorbed heat obtained from the Sun. This can be achieved as the vacuum has outstanding insulation property. Plus, the evacuated-tube collectors can perform well in cold weather compared to the flat-plate collector which suffers high heat loss under the same condition.

Martínez-Rodríguez et al. (2017) identified that the evacuated-tube collectors have multiple designs. For example, the all-glass also known as Dewar type, the all-glass fixed with coaxial pipes, the ones operating with heat pipes, the ones fitted with a U-shaped pipe and metal-glass collectors. Generally, the collector is comprised of rows of transparent glass tubes aligned in parallel and each of them contains a selective coating absorber. Normally, tin-tube design is integrated into the absorber; however, cylindrical absorber design is adopted as well (Alghoul et. al, 2017). Figure 2.6 displays the drawing of an evacuated-tube collector.

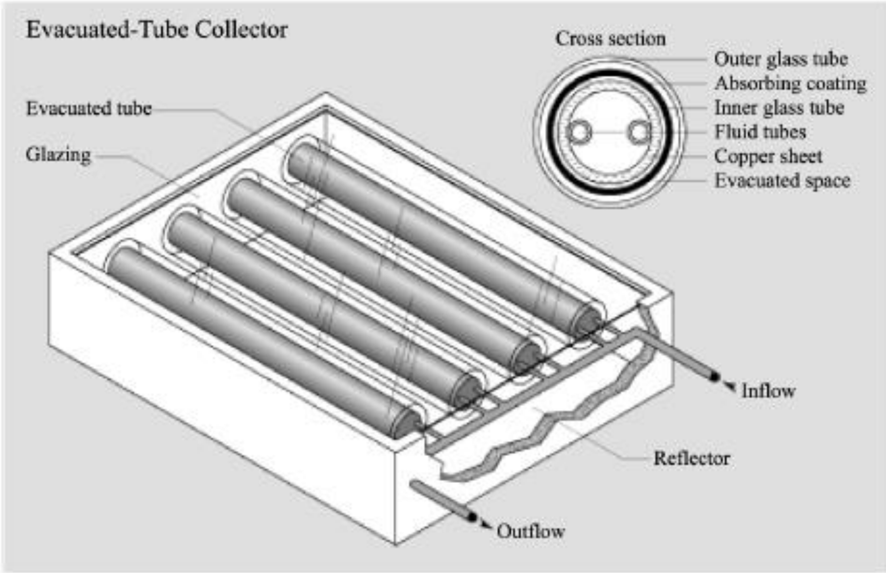

Figure 2.6: Drawing of an Evacuated-tube Collector (Alghoul et al., 2017)

There are a few downsides of using evacuated-tube collectors. Sabiha et al. (2015) reviewed that the evacuated tubes are very fragile. The main reason for its fragility is annealed glass is used to manufacture the two layers of annealed borosilicate glass. Annealed glass is less rigid compared to tempered glass. Hence, the tubes must be handled with care or else they will shatter easily. Next, overheating is another problem when evacuated-tube collectors are used. Since high temperature can be produced from these collectors, it is unwise to install evacuated-tube collectors for domestic solar water heating; they should be used for commercial purposes. Ample load is needed continuously for the domestic solar water heater system to ensure the temperature stays below 100˚C; if not then the vacuum property will be lost ultimately because of overheating. Thirdly, the cost and maintenance of evacuated-tube collectors. They are not used widely due to its high initial cost although it is simple to be manufactured.

2.3.3 Concentrating Solar Collectors

Goswami (2015) stated that when the flux incident on an aperture area, A_a was reflected or refracted onto the absorber area A_r, the solar radiation concentration is attained. The ratio of receiver's solar flux, I_r to the aperture's flux, I_a is calculated to obtain the optical concentration ratio,

$$CR_O = \frac{I_r}{I_a} \tag{2.6}$$

Then, the relevant areas can be used to calculate the geometric concentration ratio,

$$CR = \frac{A_a}{A_r} \tag{2.7}$$

The optical concentration ratio provides an accurate value. This is because optical losses from both the refracting and reflecting elements are included. The downside of this ratio is that it does not show any relevant information on thermal losses from the receiver area as it is not related to the receiver area. Concentrators possess higher efficiency than flat plate collectors at a given temperature. This is due to the smaller area where heat loss occurs. The concentration ratio for concentrators is more than 1, whereas the concentration ratio for a flat plate is about 1. On the other hand, concentrators have their disadvantages. For instance, s small portion of the diffuse energy can be harvested only at the aperture (Goswami, 2015).

CHAPTER 3

METHODOLOGY

3.1 Overview

This chapter describes the methodology applied in this study. First, the CPC design parameters are set. The CPC geometry will be obtained by using general formula. Then, the slope angle of the CPC geometry is attained by applying implicit differentiation method. The optical geometry of discrete CPC ICSSWH is then modelled by using CAD software and validated by using ray tracing software. After the optimised optical geometry design of the discrete CPC ICSSWH are determined, the mechanical structure of the discrete CPC ICSSWH will be designed and constructed. Finally, the performance of the CPC ICSSWH will be evaluated based on the experimental result. Figure 3.1 presents the flowchart of the project.

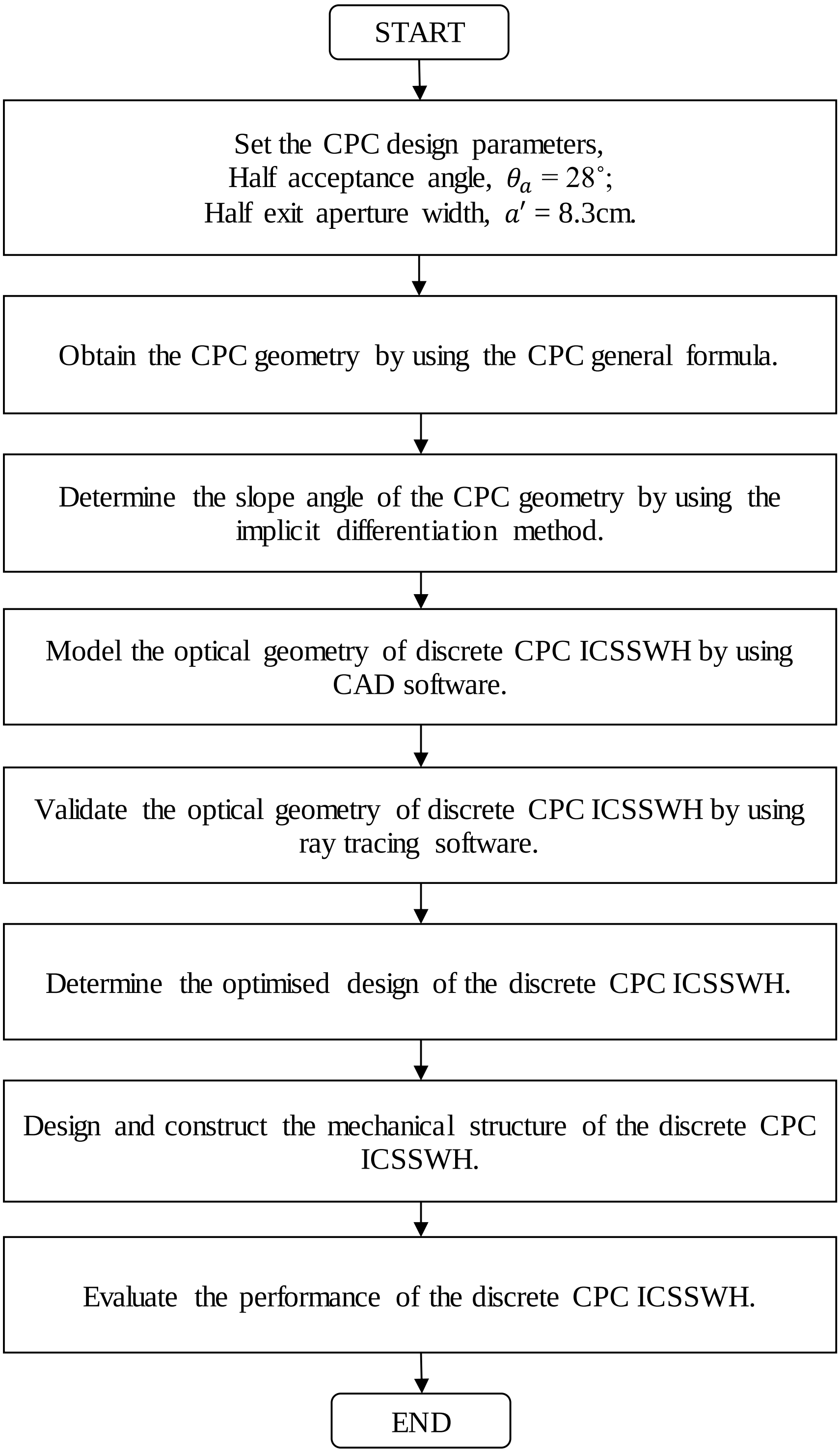

Figure 3.1: Flowchart of the Project

3.2 Optical geometry design of discrete CPC ICSSWH.

This step is vital to ensure the CPC geometry is valid prior the construction of the mechanical design of the discrete CPC ICSSWH. The CPC design parameters must be determined in order to obtain the geometry of the CPC. The general formula of the CPC will be utilised to attain the required geometry. The optical geometry of the discrete CPC ICSSWH can be obtained after the number of facet mirrors is determined. Ray tracing is used to validate the optical design of the discrete CPC ICSSWH geometry and the optimised design is chosen for construction of the discrete CPC ICSSWH.

Due to the inclination of the rotating axis of the earth, the sun declination varies from 23.45° to -23.45° throughout the entire year. In order to ensure the entire incident sun rays radiated on the absorber tank throughout the year, the half acceptance angle of the CPC plays an important role in the CPC geometrical design. As the latitude and longitude of Kampar is 4.3085˚ N, 101.1537˚ E, the minimum half acceptance angle required will be equal to the latitude plus the maximum sun declination angle which is 23.45˚ plus 4.3085˚ N equal to 28˚ after rounding off the exact value. The trough will align in east-west configuration. The half exit aperture width is also the radius of the tank.

3.2.1 Determine the CPC geometry by using CPC general formula.

The initial phase of this project is to acquire the CPC geometry by using the formula as shown in equation (3.1),

$$(x\cos\theta_a + y\sin\theta_a)^2 + 2a'(1+\sin\theta_a)^2 x - 2a'\cos\theta_a(2+\sin\theta_a)y - a'^2(1+\sin\theta_a)(3+\sin\theta_a) = 0 \quad (3.1)$$

where x is the x-coordinate of the point, y is the y-coordinate of the point, θ_a is the half acceptance angle, and a' is the half exit aperture.

The first x-coordinate is set to be the same value as the radius of the tank, then the first y-coordinate is calculated using general quadratic equation. The last y-coordinate which is also the height of the CPC is obtained using equation (3.2) and the last x-coordinate is calculated by inserting obtained last y-coordinate into equation (3.1). The half entry aperture is obtained using equation (3.3),

$$H_{cpc} = \frac{a'(1+\sin\theta_a)\cos\theta_a}{\sin^2\theta_a} \tag{3.2}$$

$$a = \frac{a'}{\sin\theta_a} \tag{3.3}$$

3.2.2 Determine the slope angle of the CPC geometry by using the implicit differentiation method.

The CPC formula is differentiated by using implicit differentiation method to get the gradient of the coordinate, as shown in equation (3.5). The gradient value is then obtained by inserting the x-coordinate and y-coordinate into it. Then, the slope angle is calculated by performing arc-tangent on the gradient value as shown in equation (3.4),

$$(slope\,angle)_{x,y} = \arctan\left(\frac{dy}{dx}\right) \tag{3.4}$$

where

$$\frac{dy}{dx} = \frac{-2x\cos^2\theta_a - 2y\sin\theta_a\cos\theta_a - 2a'(1+\sin\theta_a)^2}{2x\sin\theta_a\cos\theta_a + 2y\sin^2\theta_a - 2a'\cos\theta_a(2+\sin\theta_a)} \tag{3.5}$$

3.2.3 Design the optical geometry of discrete CPC ICSSWH.

After obtaining the slope angles of the first and last coordinates, the overall delta angle, $\Delta\theta_o$ is obtained using equation (3.6),

$$\Delta\theta_o = \theta_f - \theta_i \tag{3.6}$$

where θ_f is the final slope angle and θ_i is the first slop angle.

The delta angle, $\Delta\theta_m$ that can be allocated for each mirror is obtained using equation 3.7,

$$\Delta\theta_m = \frac{\Delta\theta_o}{n_{mirror}} \tag{3.7}$$

where n_{mirror} is the number of mirrors.

For the first trial, the number of facet mirrors was set to ten pieces on each side of the CPC geometry. The top edge slope angle for the first mirror is calculated using equation (3.8), then the top edge slope angle for the first mirror was then acted as the bottom edge slope angle for the second mirror and the same approach was applied to the subsequent mirrors. The x-coordinate and y-coordinate of the top edge of the mirrors were calculated by performing substitution method on equation 3.4 and equation 3.1.

$$\theta_n = \theta_i + n_{mirror}(\Delta\theta_m) \tag{3.8}$$

After that, the width of the facet, which is also the hypotenuse of the triangle was calculated by using Pythagorean Theorem as shown in equation 3.9,

$$hypotenuse = \sqrt{(\Delta x)^2 + (\Delta y)^2} \tag{3.9}$$

where Δx is the difference in x-coordinates between the top edge and bottom edge of the mirror and Δy is the difference in y-coordinates between the top edge and bottom edge of the mirror.

The facet mirrors are then joined together to form a discrete CPC. The steps were repeated for the subsequent trials with different sets of the number of mirrors on each side of the discrete CPC which are five, three, and two mirrors. SolidWorks is used to model the optical geometry of the discrete CPC ICSSWH. Figures 3.2 display the different complete sets of optical designs of the discrete CPC ICSSWH. Tables 3.1 exhibit the parameters of the complete sets of optical designs of the discrete CPC ICSSWH.

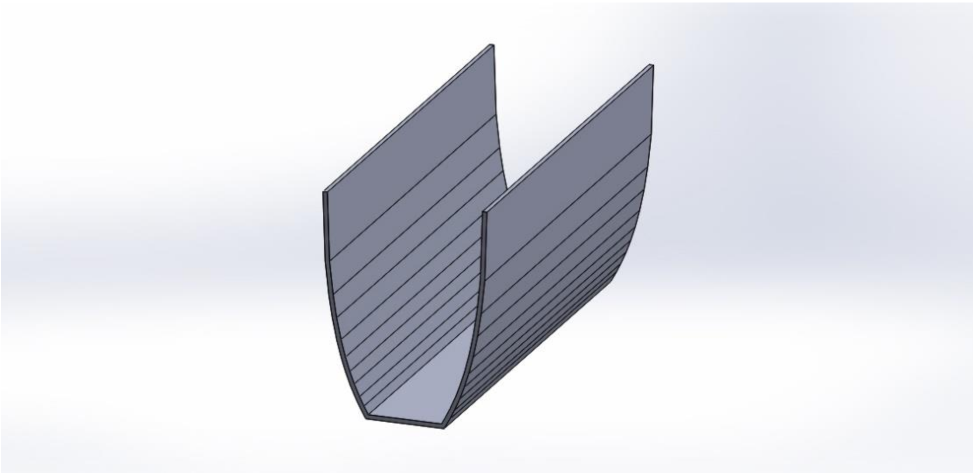

Figure 3.2(a)

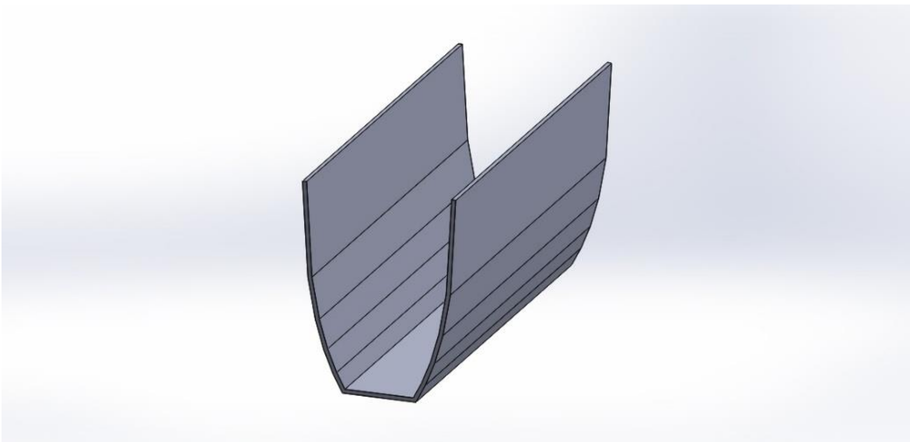

Figure 3.2(b)

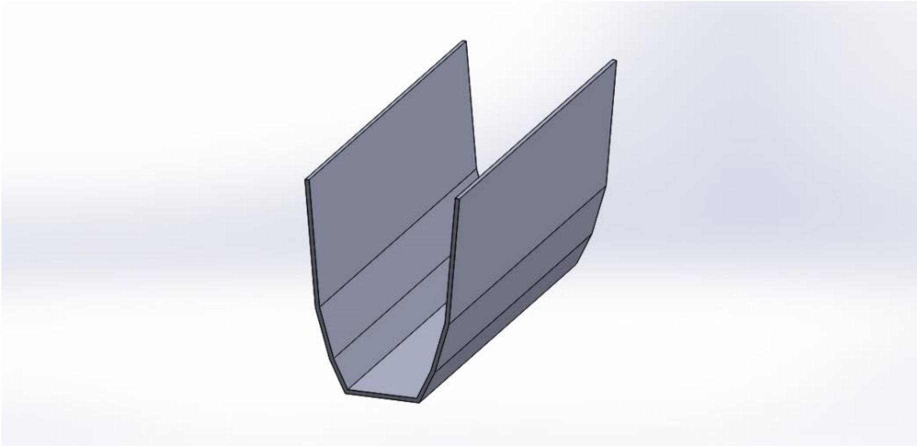

Figure 3.2(c)

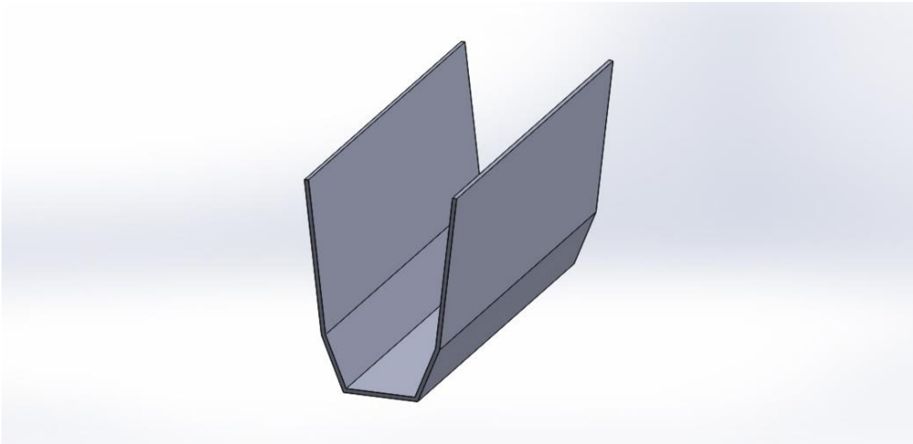

Figure 3.2(d)

Figure 3.2: Complete Optical Design of the Discrete CPC ICSSWH with Different Sets of the Number of Mirrors. (a) 10 Mirrors, (b) 5 Mirrors, (c) 3 Mirrors, and (d) 2 Mirrors

Table 3.1: The Parameters of the Complete Sets of Optical Designs of the Discrete CPC ICSSWH with Different Sets of the Number of Mirrors. (a) 10 mirrors, (b) 5 mirrors, (c) 3 mirrors, and (d) 2 mirrors.

Table 3.1(a)

Mirror Number	Bottom edge mirror's *x*-coordinate (cm)	Top edge mirror's *x*-coordinate (cm)	Δ*x* (cm)	Bottom edge mirror's *y*-coordinate (cm)	Top edge mirror's *y*-coordinate (cm)	Δ*y* (cm)	Bottom edge mirror's slope angle (°)	Top edge mirror's slope angle (°)	Hypotenuse (cm)	New Slope Angle (°)
1	8.3	9.3	1.0	0.0	1.8	1.8	59.00	61.86	2.1	60.9
2	9.3	10.3	1.0	1.8	3.8	2.0	61.86	64.70	2.2	63.4
3	10.3	11.5	1.2	3.8	6.5	2.7	64.70	68.09	3.0	66.0
4	11.5	12.5	1.0	6.5	9.2	2.7	68.09	70.91	2.9	69.7
5	12.5	13.5	1.0	9.2	12.3	3.1	70.91	73.75	3.3	72.1
6	13.5	14.5	1.0	12.3	16.1	3.8	73.75	76.63	3.9	75.3
7	14.5	15.5	1.0	16.1	20.9	4.8	76.63	79.65	4.9	78.2
8	15.5	16.3	0.8	20.9	26.0	5.1	79.65	82.27	5.2	81.1
9	16.3	17.1	0.8	26.0	33.4	7.4	82.27	85.38	7.4	83.8
10	17.1	17.6	0.5	33.4	48.9	15.5	85.38	88.44	15.5	88.2

Table 3.1(b)

Mirror Number	Bottom edge mirror's *x*-coordinate (cm)	Top edge mirror's *x*-coordinate (cm)	Δ*x* (cm)	Bottom edge mirror's *y*-coordinate (cm)	Top edge mirror's *y*-coordinate (cm)	Δ*y* (cm)	Bottom edge mirror's slope angle (°)	Top edge mirror's slope angle (°)	Hypotenuse (cm)	New Slope Angle (°)
1	8.3	10.3	2.0	0.0	3.8	3.8	59.00	64.70	4.3	62.2
2	10.3	12.5	2.2	3.8	9.2	5.4	64.70	70.91	5.8	67.8
3	12.5	14.5	2.0	9.2	16.1	6.9	70.91	76.63	7.2	73.8
4	14.5	16.3	1.8	16.1	26.0	9.9	76.63	82.27	10.1	79.7
5	16.3	17.6	1.3	26.0	48.9	22.9	82.27	88.44	22.9	86.8

Table 3.1(c)

Mirror Number	Bottom edge mirror's *x*-coordinate (cm)	Top edge mirror's *x*-coordinate (cm)	Δ*x* (cm)	Bottom edge mirror's *y*-coordinate (cm)	Top edge mirror's *y*-coordinate (cm)	Δ*y* (cm)	Bottom edge mirror's slope angle (°)	Top edge mirror's slope angle (°)	Hypotenuse (cm)	New Slope Angle (°)
1	8.3	11.7	3.4	0.0	7.0	7.0	59.00	68.66	7.8	64.1
2	11.7	15.1	3.4	7.0	18.8	11.8	68.66	78.42	12.3	73.9
3	15.1	17.6	2.5	18.8	48.9	30.1	78.42	88.44	30.2	85.3

Table 3.1(d)

Mirror Number	Bottom edge mirror's *x*-coordinate (cm)	Top edge mirror's *x*-coordinate (cm)	Δ*x* (cm)	Bottom edge mirror's *y*-coordinate (cm)	Top edge mirror's *y*-coordinate (cm)	Δ*y* (cm)	Bottom edge mirror's slope angle (°)	Top edge mirror's slope angle (°)	Hypotenuse (cm)	New Slope Angle (°)
1	8.3	13.5	5.2	0.0	12.3	12.3	59.00	73.75	13.4	67.1
2	13.5	17.6	4.1	12.3	48.9	36.6	73.75	88.44	36.8	83.6

3.2.4 Ray-tracing simulation of discrete CPC ICSSWH.

The SolidWorks files that contain the designs of the optical geometry of the discrete CPC ICSSWH are then saved as Initial Graphics Exchange Specification (IGES) files. IGES files allow the user to open the 3D design using different Computer Aided Design (CAD) software. Those IGES files are then imported to TracePro, a ray tracing software to simulate and validate the optical geometry of discrete CPC ICSSWH. However, as the system is a trough, 2D ray-tracing will be sufficient. Furthermore, 2D ray tracing on the optical geometry of the discrete CPC ICSSWH is more than enough to study whether the simulated sun rays can completely enter it without being reflected out.

Initially, an absorber tank was added 5mm above the base mirror. Figure 3.3 displays the graphic user interface (GUI) of inserting the absorber tank. The property of the outer surface of the cylinder is changed to “perfect absorber”. Figure 3.4 shows the GUI of the updated property of the absorber tank. “Mirror” was applied as the property of the facet mirrors. Figure 3.5 shows the GUI of the updated property of the facet mirrors.

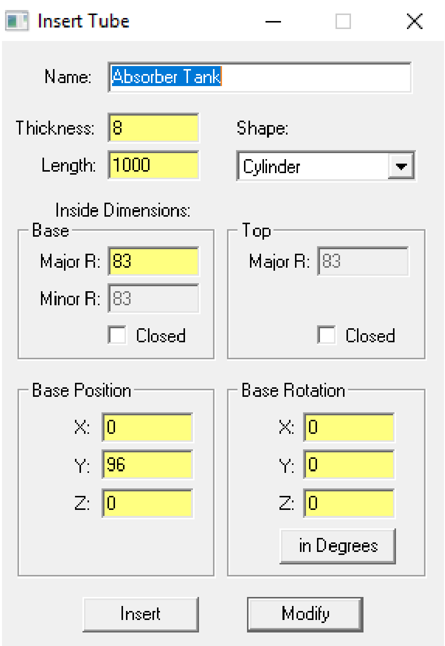

Figure 3.3: GUI of Inserting the Absorber Tank

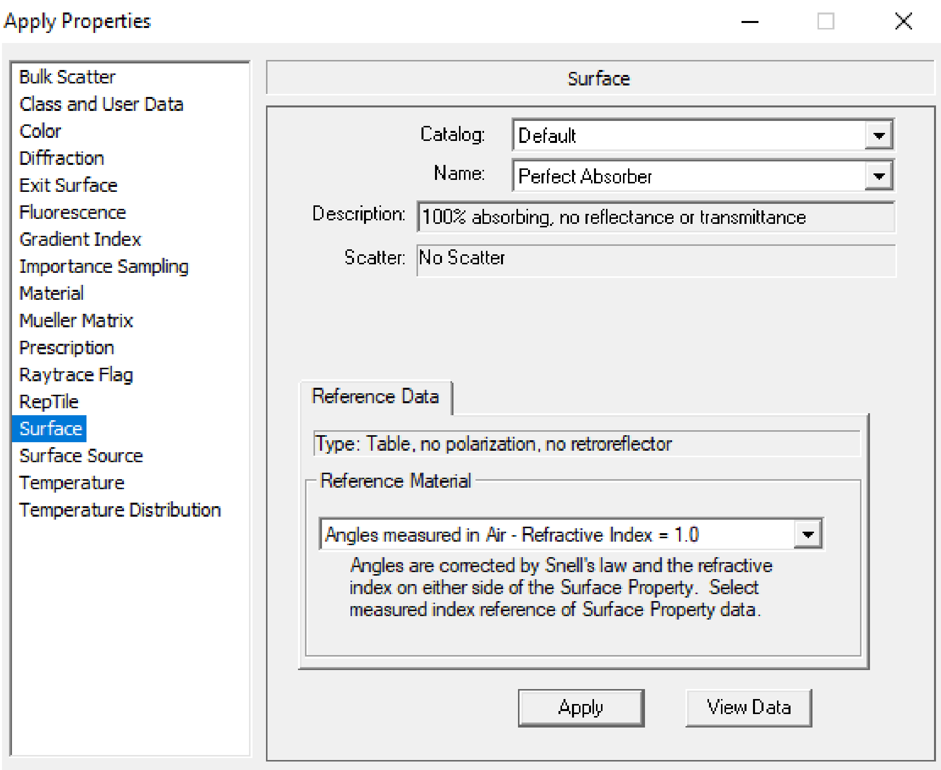

Figure 3.4: GUI Displays the Absorber Tank's Property as Perfect Absorber

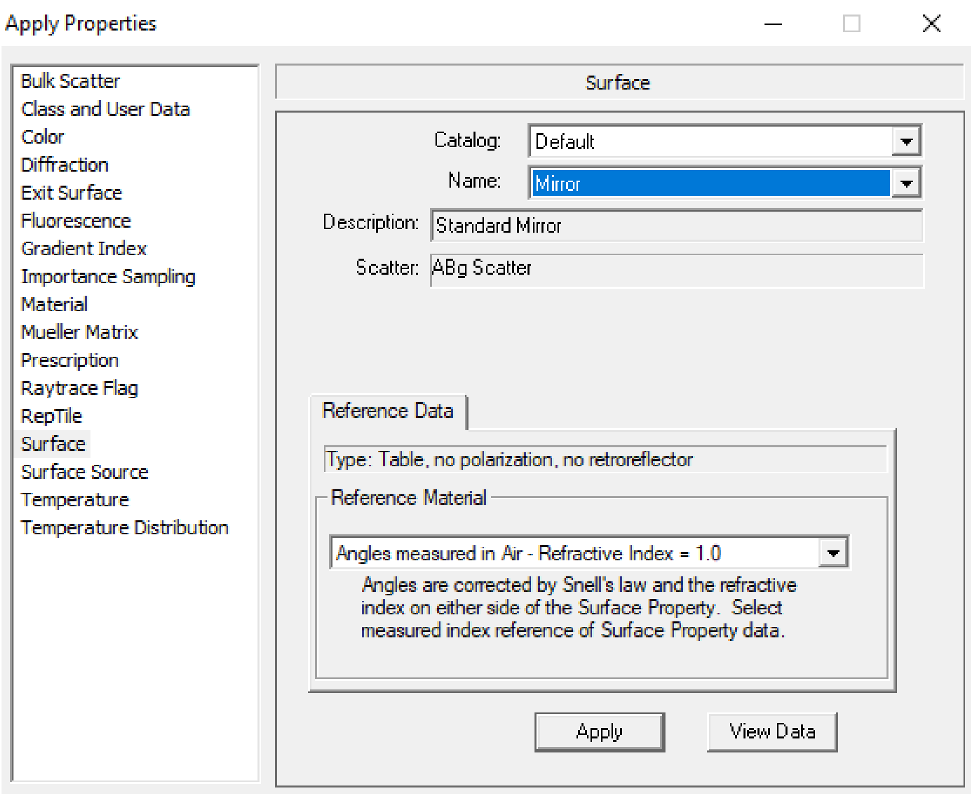

Figure 3.5: GUI Displays the Facet Mirrors' Property as Mirror

After the properties of the optical geometry of discrete CPC ICSSWH were determined accordingly, the grid source, which is the sun is defined. The grid boundary is set where Y half-height is 300mm, and X half-width is 5mm in order to fully cover the aperture of the system. The grid pattern is set to rectangular and the Y points and X points are set to 50 and 1 respectively in which the multiplication of both points represents the total incoming rays. The irradiance value is set to 1000W/m^2. The origin values of X, Y, and Z are set as shown in Figure 3.6 to ensure the grid source is on top of the optical geometry of discrete CPC ICSSWH. Then, the Y-normal vector is set to -1 to ensure the sun rays radiated downwards. The X-up vector is set to 1 as normal ground.

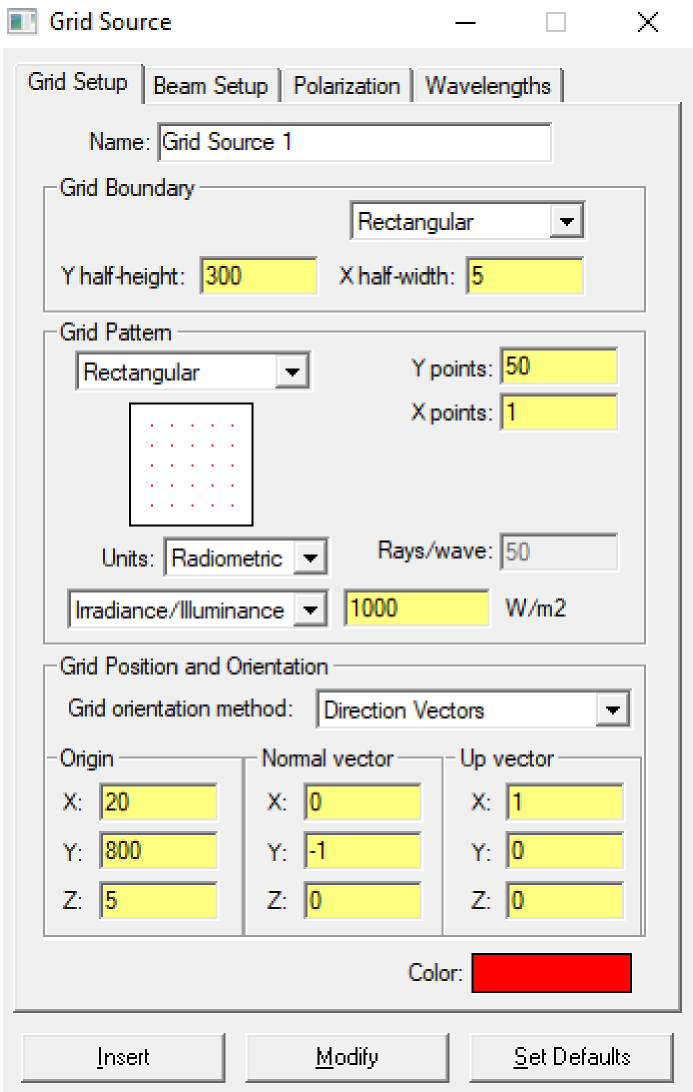

Figure 3.6: GUI Shows the Parameters of the Grid Source

Different incident angles are simulated to study and ensure the incident sun rays enter the discrete CPC ICSSWH completely. The mentioned incident angles from y-axis are 0˚, 5˚, 10˚, 15˚, 20˚, 25˚, and 28˚. Figures 3.7 display the ray tracing of the design with 10 mirrors at one side of the geometry at different incident angles respectively. Next, Figures 3.8 display the ray tracing of the design with 5 mirrors at one side of the geometry at different incident angles respectively. Then, Figures 3.9 display the ray tracing of the design with 3 mirrors at one side of the geometry at different incident angles respectively. Next, Figures 3.10 display the ray tracing of the design with 2 mirrors at one side of the geometry at different incident angles respectively.

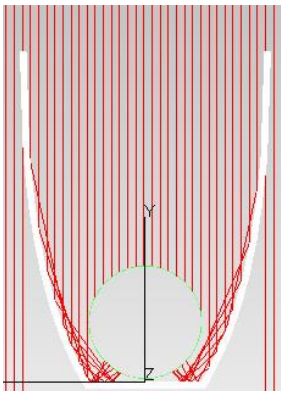

Figure 3.7(a)

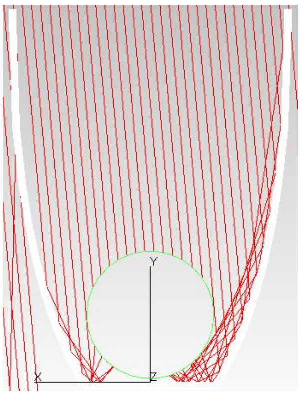

Figure 3.7(b)

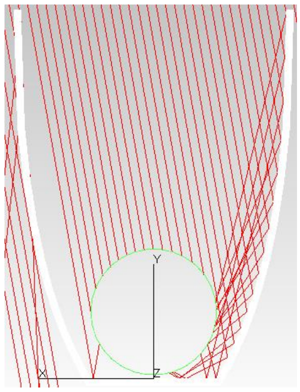

Figure 3.7(c)

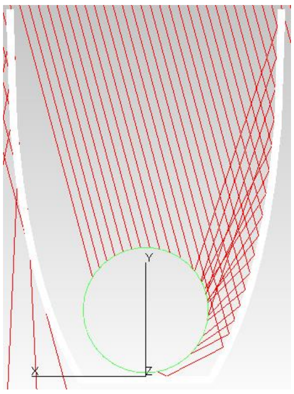

Figure 3.7(d)

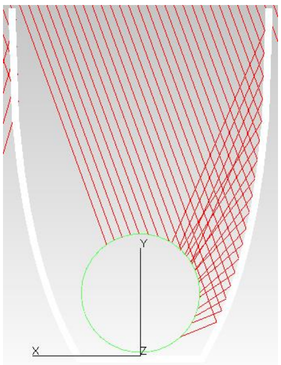

Figure 3.7(e)

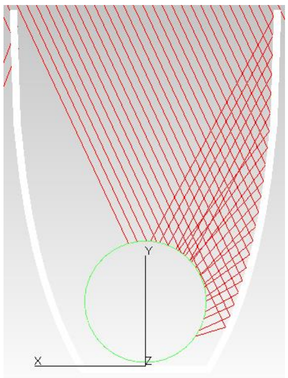

Figure 3.7(f)

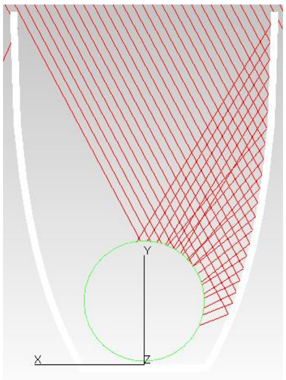

Figure 3.7(g)

Figure 3.7: Ray Tracing of the Optical Design of Discrete CPC ICSSWH with 10 Mirrors at One Side of the Geometry at Different Incident Angles. (a) 0˚, (b) 5˚, (c) 10˚, (d) 15˚, (e) 20˚, (f) 25˚, and (g) 28˚

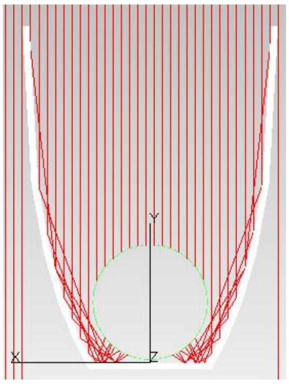

Figure 3.8(a)

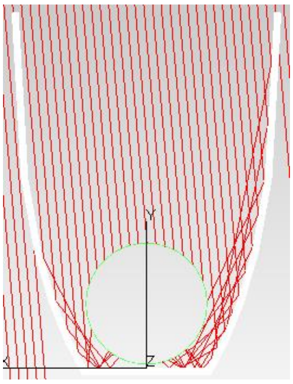

Figure 3.8(b)

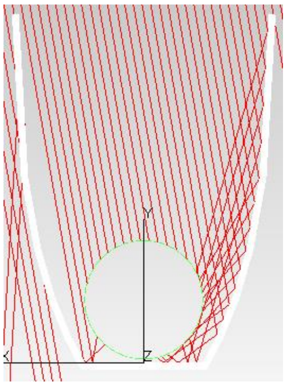

Figure 3.8(c)

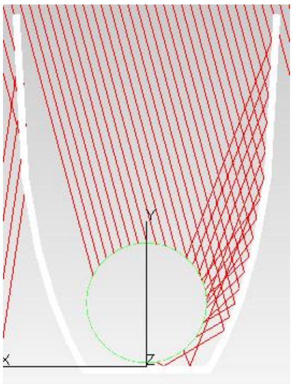

Figure 3.8(d)

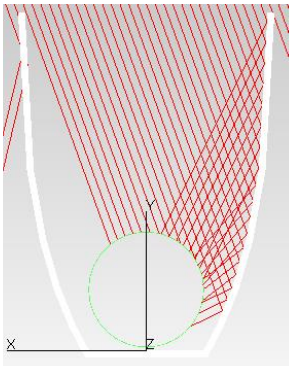

Figure 3.8(e)

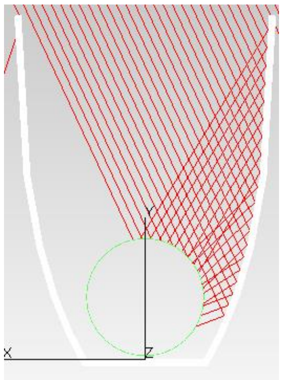

Figure 3.8(f)

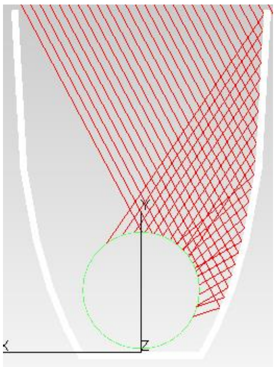

Figure 3.8(g)

Figure 3.8: Ray Tracing of the Optical Design of Discrete CPC ICSSWH with 5 Mirrors at One Side of the Geometry at Different Incident Angles. (a) 0˚, (b) 5˚, (c) 10˚, (d) 15˚, (e) 20˚, (f) 25˚, and (g) 28˚

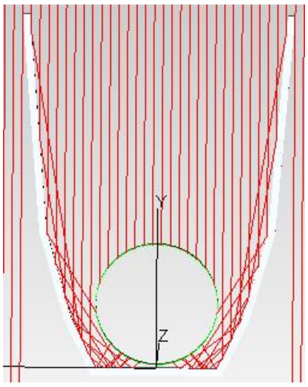

Figure 3.9(a)

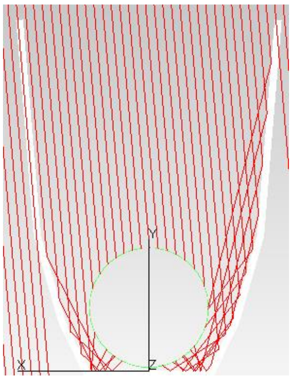

Figure 3.9(b)

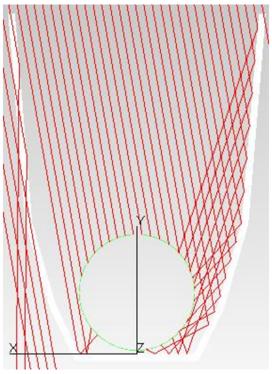

Figure 3.9(c)

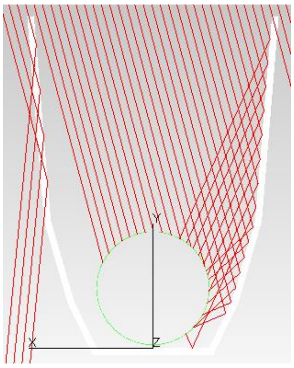

Figure 3.9(d)

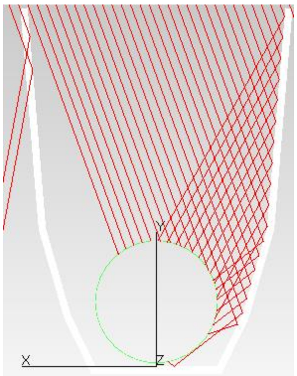

Figure 3.9(e)

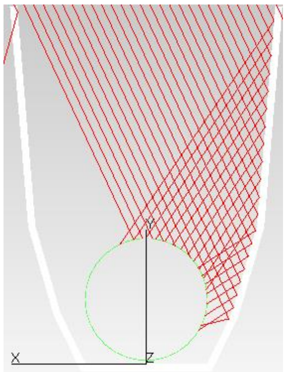

Figure 3.9(f)

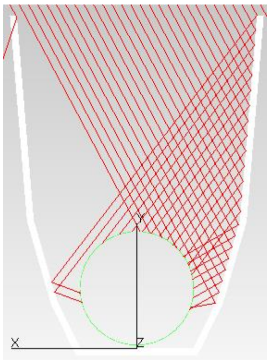

Figure 3.9(g)

Figure 3.9: Ray Tracing of the Optical Design of Discrete CPC ICSSWH with 3 Mirrors at One Side of the Geometry at Different Incident Angles. (a) 0˚, (b) 5˚, (c) 10˚, (d) 15˚, (e) 20˚, (f) 25˚, and (g) 28˚

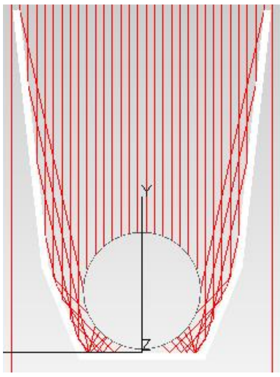

Figure 3.10(a)

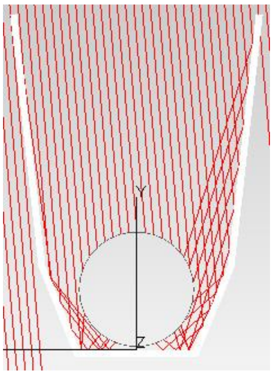

Figure 3.10(b)

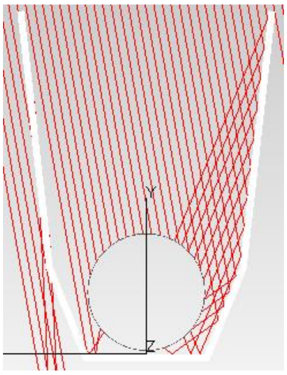

Figure 3.10(c)

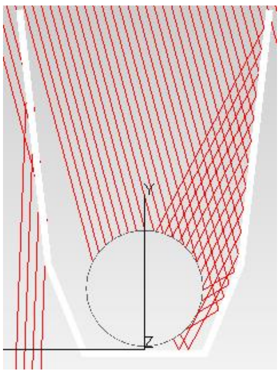

Figure 3.10(d)

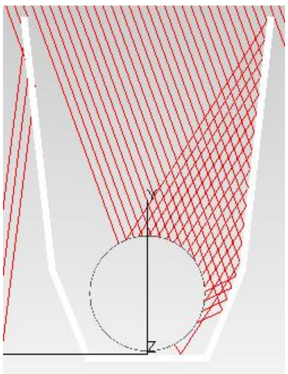

Figure 3.10(e)

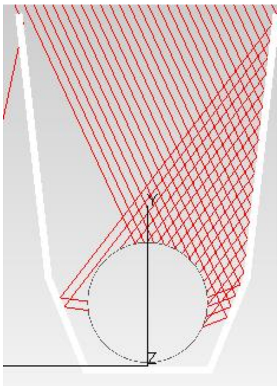

Figure 3.10(f)

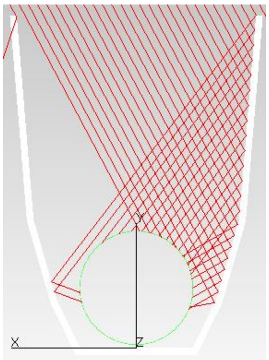

Figure 3.10(g)

Figure 3.10: Ray Tracing of the Optical Design of Discrete CPC ICSSWH with 2 Mirrors at One Side of the Geometry at Different Incident Angles. (a) 0°, (b) 5°, (c) 10°, (d) 15°, (e) 20°, (f) 25°, and (g) 28°

3.2.5 Determine the optimised optical design of the discrete CPC ICSSWH.

Based on the results obtained from the ray tracing simulation, the optimised optical design of the discrete CPC ICSSWH, which has the lowest possible number of facet mirrors, is chosen. This is to ensure that the prototype is easy to be fabricated since the design has lower complexity compared to the available CPC ICSSWH on the market. Figure 3.11 displays the optimised 2D optical design of the discrete CPC ICSSWH with the mirrors' respective parameters. Table 3.2 presents the length and the inclination angle of different mirrors.

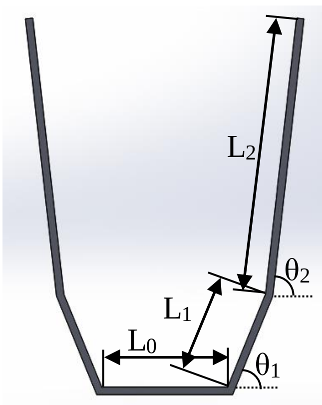

Figure 3.11: Optimised 2D optical design of the discrete CPC ICSSWH with the mirrors' respective parameters

Table 3.2: Length and Inclination Angle for Different Mirrors

Number	Mirror	Length (mm)	Inclination Angle (°)
0	Base	166	0.0
1	Lower	134	67.1
2	Upper	368	83.6

3.3 Design and construct the mechanical structure of discrete CPC ICSSWH.

SolidWorks is used to design the 3D model of the discrete CPC ICHSSWH. The parts that comprise the whole discrete CPC ICSSWH are facet mirrors, absorber tank with ball valves, wooden covers, acrylic sheets and clear float glass. All of the parts were designed separately prior to their assembly to ease the design process. Figure 3.12 shows the technical drawing of the absorber tank and Figure 3.13 displays the technical drawing of the whole assembly.

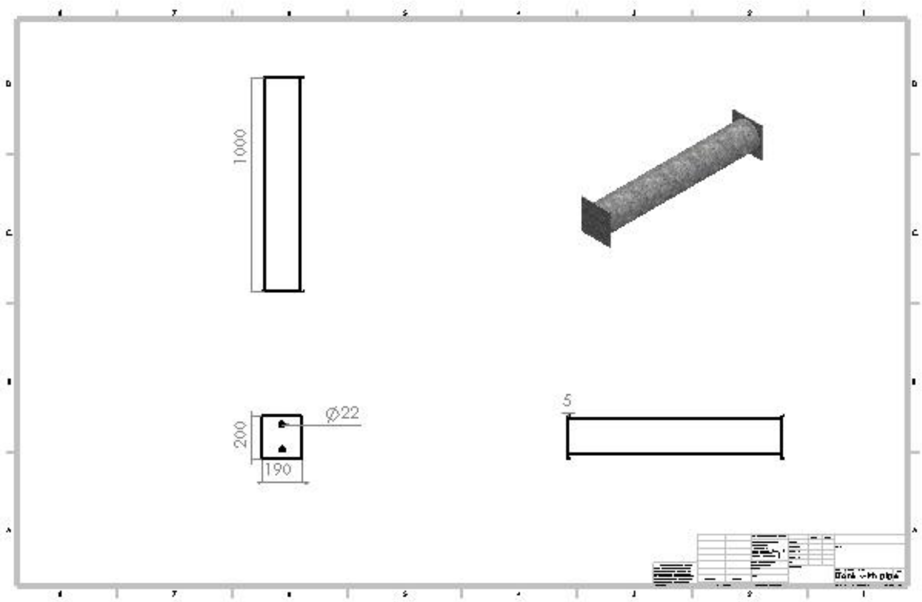

Figure 3.12: The Technical Drawing for the Absorber Tank

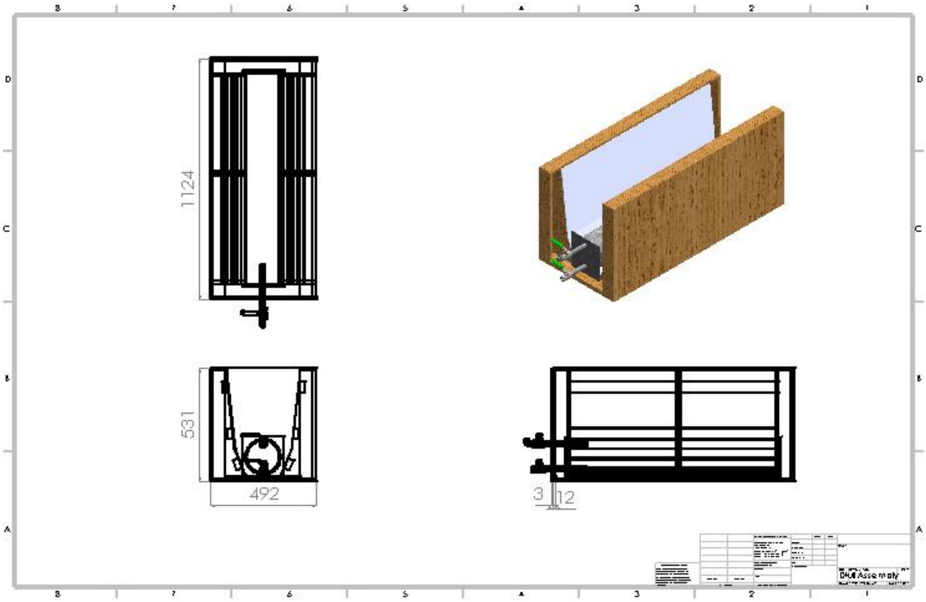

Figure 3.13: The Technical Drawing for the Full Assembly of the Discrete CPC ICSSWH

For the actual assembly of the design, the discrete CPC ICSSWH system prototype was fabricated in Universiti Tunku Abdul Rahman, Kampar with latitude 4.3085˚ N and longitude 101.1537˚ E. The discrete CPC was designed to allow sunlight concentrate on the absorber tank and enables the conversion of solar energy into thermal energy. The specifications of the components of the discrete CPC ICSSWH system and methods to fabricate the components are delineated in the following section.

3.3.1 Mirrors

The discrete CPC was constructed by using sets of rectangular facet mirrors. The base of the discrete CPC was constructed by using two rectangular facet mirrors with dimension of 515 mm (length) × 166 mm (width) × 3 mm (thickness) and 465 mm (length) × 166 mm (width) × 3 mm (thickness) respectively. The upper half of the discrete CPC was constructed by using two rectangular facet mirrors with dimension of 515 mm (length) × 368 mm (width) × 3 mm (thickness) and 465 mm (length) × 368 mm (width) × 3 mm (thickness) respectively on each side of the discrete CPC.

The total length of the mirrors is 980mm. The upper facet mirrors are inclined at the angle of 83.6˚ relative to the base facet mirrors. Meanwhile, the lower half of the discrete CPC was constructed by using two rectangular facet mirrors with dimension of 515 mm (length) × 134 mm (width) × 3 mm (thickness) and 465 mm (length) × 134 mm (width) × 3 mm (thickness) respectively on each side of the discrete CPC. The lower facet mirrors are inclined at the angle of 67.1˚ relative to the base facet mirrors. Figure 3.14 shows the mirrors attached to the supporting frame.

Figure 3.14: Mirrors Attached to the Supporting Frame

3.3.2 Wooden Cradle

A wooden cradle was made to support the facet mirrors. Two sheets of plywood with a dimension of 4 ft × 8 ft x 12 mm are used to construct the wooden cradle. Plywood is used because it has low thermal conductivity of 0.13 W/(mK). Eight facet mirror supporting frames were sketched accurately according to the dimension as shown in Figure and sawed. The facet mirror supporting frames were then interlocked by timber strips with dimension of 1 inch × 2 inches x 980 mm to further support the facet mirrors. Figure 3.15 shows the supporting frame with the timber strips interlocked together. The facet mirrors were bonded to the timber strips using adhesive. A rectangular base plywood with dimension of 166 mm (width) × 980 mm (length) x 12 mm (thickness) is used as the facet mirror supporting base. The supporting frame is then covered by side plywood cover (1100 mm × 528 mm), front plywood cover (492 mm × 528 mm), and base cover (1100 mm × 468 mm). Shellac was applied three times to the trimmed plywood sheets prior to the assembly of the wooden cradle for water protection. Figure 3.16 shows the wooden cradle with mirrors.

Figure 3.15: Supporting Frames with Timber Strips Interlocked Together

Figure 3.16: Wooden Cradle with Mirrors

3.3.3 Absorber Tank

A tank of 17671 cm^3 (17.671 litres) was built by welding two pieces of metal plates to both side of a galvanised iron pipe. Two holes were drilled at one of the metal plate for piping purposes. The hole at the bottom acts as inlet line to allow water flows in whereas the hole at the top serves as outlet line to allow pressure in the tank to be relieved. The whole surface of the tank was sprayed in black colour in order to increase its solar irradiance absorptivity. The tank acts as both storage and absorber tank, hence it cannot be insulated but its surrounding space can be insulated for better thermal resistance. Figure 3.17 displays the absorber tank.

Figure 3.17: Absorber Tank

3.3.4 Glazing Cover

Polystyrene boards are placed in the gap between the side cover and the facet mirrors to provide thermal insulation. It is also used due to its cost effective and low thermal conductivity of 0.035 W/(mK). Air gap also exists between the polystyrene boards to further enhance the thermal resistance. Clear float glass and acrylic sheets were used as glazing material to minimise the heat losses from convection. The acrylic sheets with the dimension of 531 mm × 492 mm × 3 mm were screwed to the front cover of the wooden cradle respectively. Meanwhile, clear float glass with the dimension of 1124 mm × 492 mm x 5 mm was fixed on top of the wooden cradle with silicon adhesive. With that, the space within the system is fully insulated. Figure 3.18 shows the 3D model of the discrete CPC ICSSWH. Figures 3.19 displays the top and front side of the actual prototype of the discrete CPC ICSSWH.

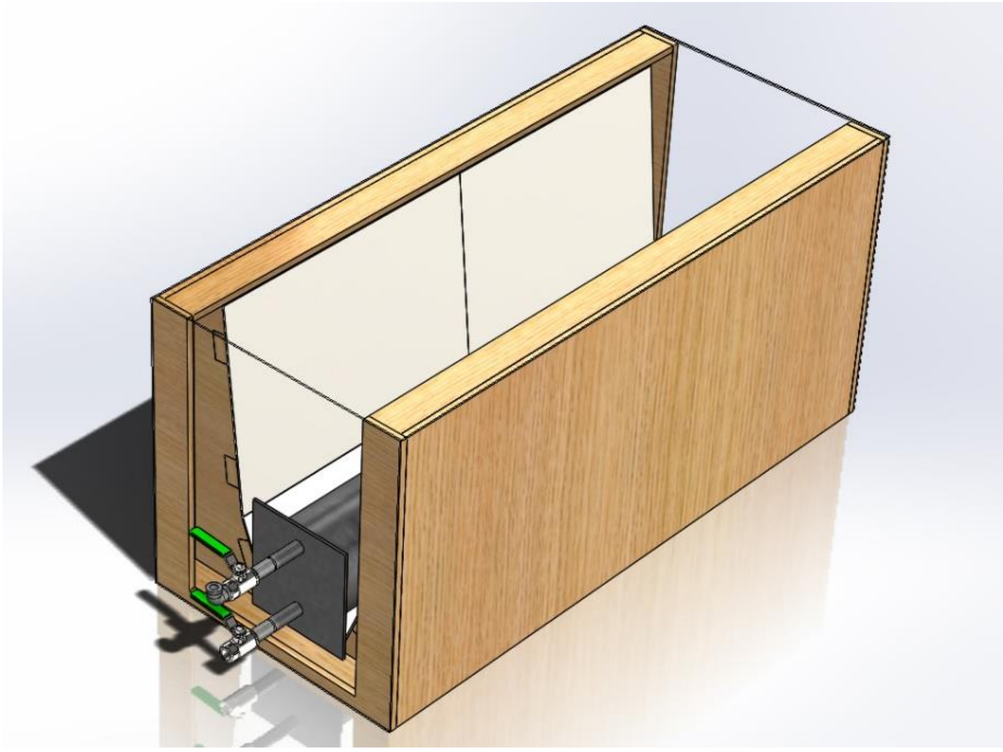

Figure 3.18: 3D Model of the Discrete CPC ICSSWH

(a)

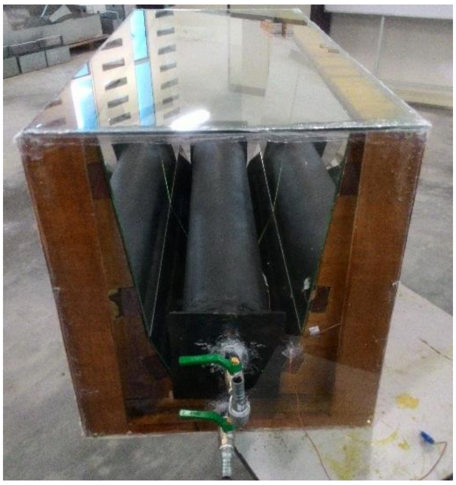

(b)

Figure 3.19: Actual Prototype of the Discrete CPC ICSSWH. (a) Top Side, (b) Front Side

3.4 Discrete CPC ICSSWH system performance evaluation.

The performance of the discrete CPC ICSSWH is evaluated by measuring the temperatures at several locations. The mentioned locations are the water, tank surface, and ambient. Type-T thermocouples and thermocouple readers are used to determine the temperatures and 5 minutes is set as the time interval to obtain the temperatures data. Prior to the data collection, the thermocouples are calibrated to obtain the instrument error. T_1 is the thermocouple for the measurement of the water temperature, T_2 is the thermocouple for the measurement of the tank surface temperature, and T_3 is the thermocouple for the measurement of the ambient temperature. Furthermore, the global horizontal irradiance(GHI) is also obtained by using pyranometer and the time interval to take GHI data is 1 minute. Figure 3.20 displays the water, tank, and ambient temperature data collection.

Figure 3.20: Water, Tank Surface, and Ambient Data Collection

CHAPTER 4

RESULTS AND DISCUSSIONS

4.1 System Performance Analysis

The discrete CPC ICSSWH was tested for its performance on different days. The water temperature in the absorber tank, tank surface temperature, ambient temperature, and the global solar irradiance were measured with respect to the local clock time. Figures 4.1 display the measurement results of water temperature in absorber tank, tank surface temperature, ambient temperature and global solar irradiance against local clock time on different day.

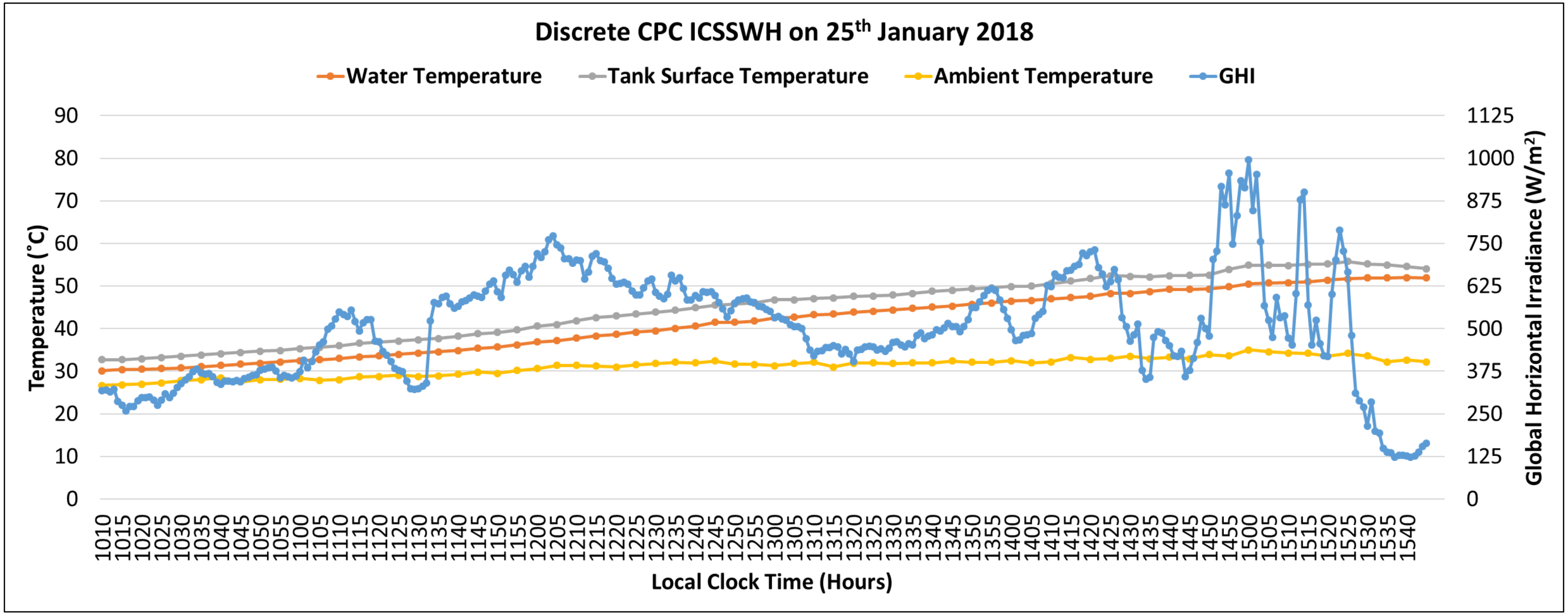

Discrete CPC ICSSWH on 25th January 2018
Water Temperature
Tank Surface Temperature
Ambient Temperature
GHI
Temperature (˚C)
Global Horizontal Irradiance (W/m2)
Local Clock Time (Hours)

Figure 4.1 (a)

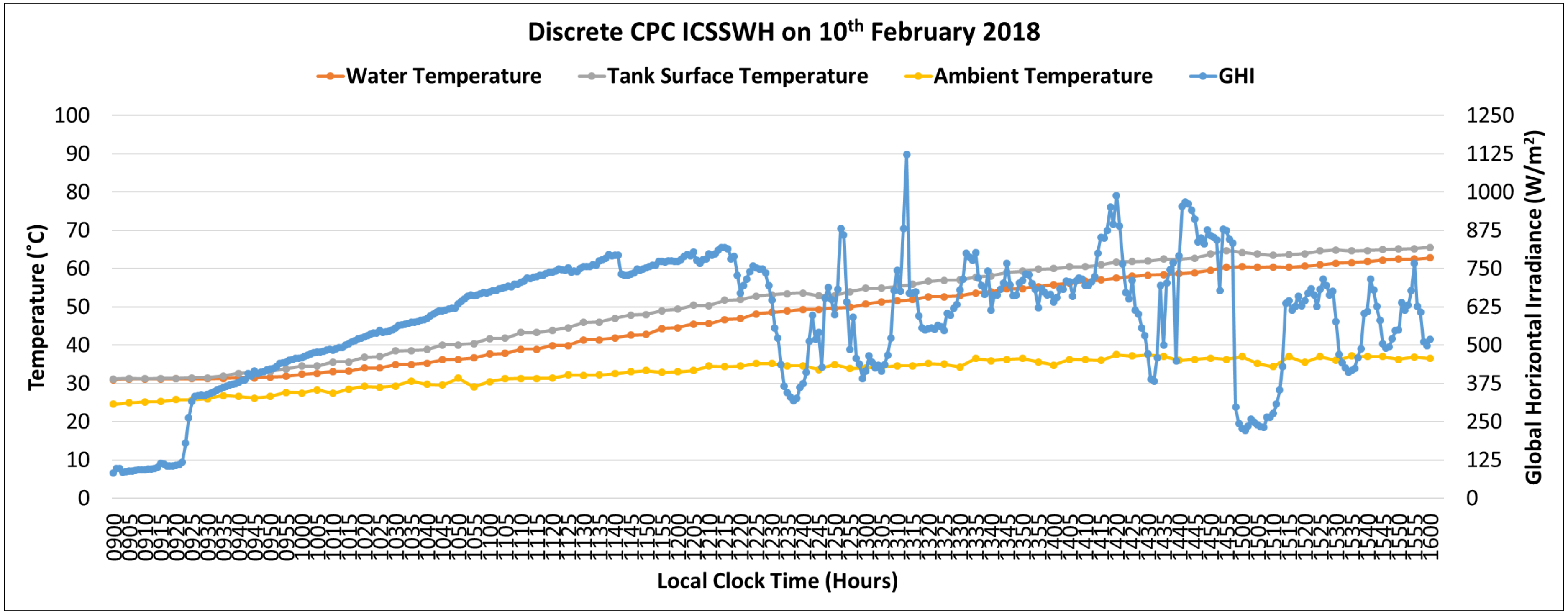
Discrete CPC ICSSWH on 10th February 2018
Water Temperature
Tank Surface Temperature
Ambient Temperature
GHI
Temperature (˚C)
Global Horizontal Irradiance (W/m2)
Local Clock Time (Hours)

Figure 4.1 (b)

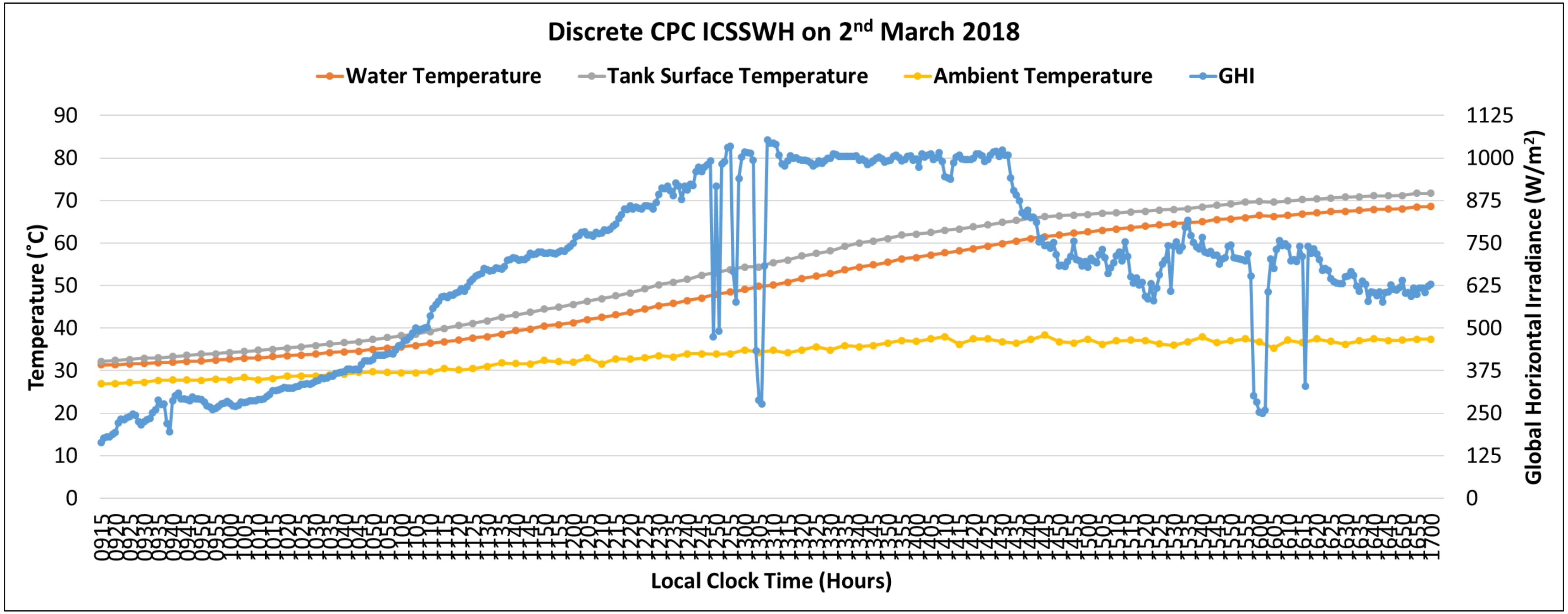
Discrete CPC ICSSWH on 2nd March 2018
Water Temperature
Tank Surface Temperature
Ambient Temperature
GHI
Temperature (°C)
Global Horizontal Irradiance (W/m2)
Local Clock Time (Hours)
90
80
70
60
50
40
30
20
10
0
1125
1000
875
750
625
500
375
250
125
0

Figure 4.1 (c)

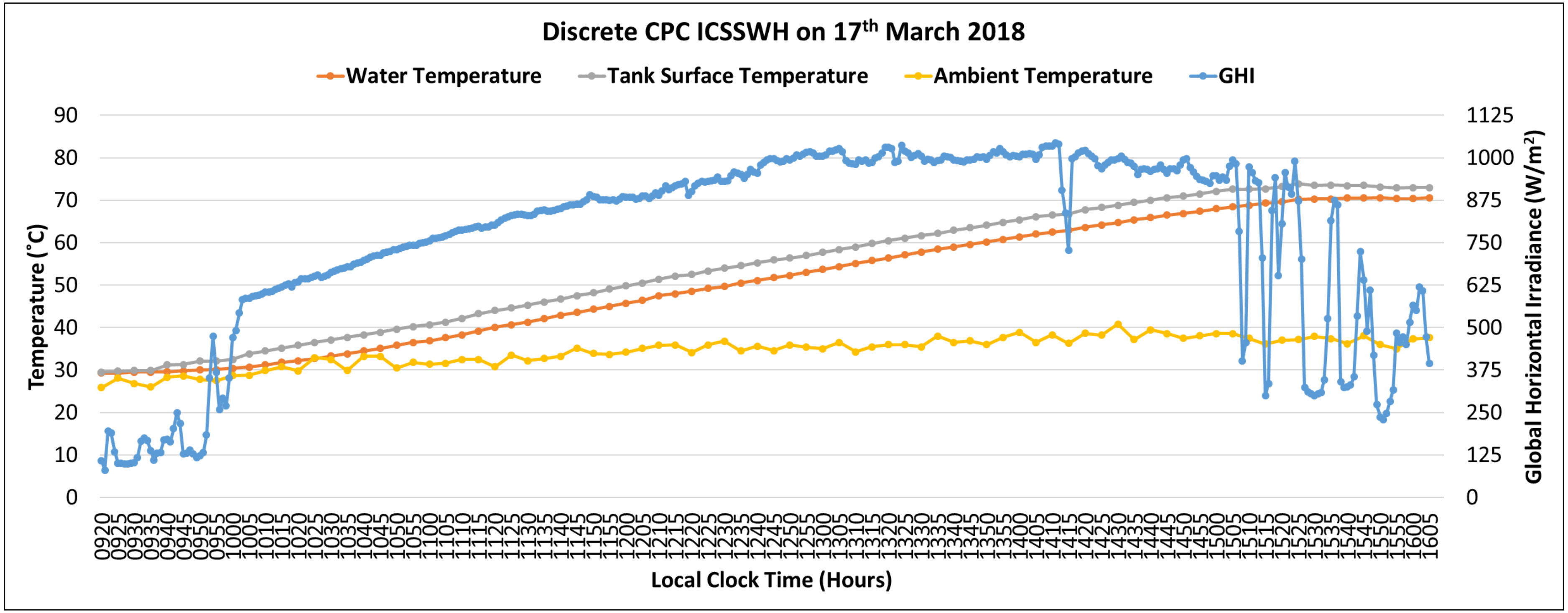

Figure 4.1(d)

Figure 4.1: Measurement Results of Water Temperature in Absorber Tank, Tank Surface Temperature, Ambient Temperature and Global Solar Irradiance against Local Clock Time. (a) 25th January 2018 (b) 10th February 2018 (c) 2nd March 2018 (d) 17th March 2018

Based on the measurement results, before the solar rays start to radiate on the absorber tank on early morning, it can be observed the temperature difference between the absorber tank surface and the water is small. When the solar rays started to radiate on the absorber tank, the temperature difference between the absorber tank and the water increases. The tank surface temperature is always higher than the water temperature throughout the experiment. This is because the storage tank which is also acts as the absorber tank will absorb the solar energy first, then only the heat energy is transferred to the water via natural convection. When the global solar irradiance dropped on evening, the temperature difference between the tank surface and water dropped. This is because the energy absorbed from the solar irradiance is almost equivalent to the heat loss to the surrounding, hence the temperatures for both the tank surface and the water remained constant. The maximum water temperature attained on 25th January 2018, 10th February 2018, 2nd March 2018 and 17th March 2018 are 52.0°C, 62.8°C, 68.6°C and 70.6°C respectively. The maximum tank surface temperature obtained on 25th January 2018, 10th February 2018, 2nd March 2018 and 17th March 2018 are 55.8°C, 65.5°C, 71.7°C and 73.9°C respectively.

Table 4.1 shows the specification of the discrete CPC ICSSWH fabricated in Universiti Tunku Abdul Rahman (Kampar Campus).

Table 4.1: The Specification of the Discrete CPC ICSSWH fabricated in Universiti Tunku Abdul Rahman (Kampar Campus)

Description	Feature/ Value
Type of reflector	Low iron silver coating mirror
Dimension of each mirror	Base mirror: 166 mm (width) × 980 mm (length) × 3mm (thickness); Lower mirror: 134 mm (width) × 980 mm (length) × 3mm (thickness); Upper mirror: 368 mm (width) × 980 mm (length) × 3mm (thickness)
Total number of mirrors	5
Inclined angle of each mirror	Base mirror: 0.0°; Lower mirror: 67.1°; Upper mirror: 83.6°
Total reflective area of discrete CPC collector	1.15m^2

Dimension of glazing cover	1124 mm (length) × 492 mm (width) × 5mm (thickness)
Dimension of absorber tank	150 mm (inner diameter) × 1000 mm (length) × 8 mm (thickness)
Total entry aperture size	0.354 m^2
Total volume of water in the storage tank	17.67 L
Orientation of the prototype	Along east-west direction
Latitude	4.31 °N
Longitude	101.15°E

To further evaluate the performance of the discrete CPC ICSSWH, several formulae as shown in the following were applied. The entire amount of solar energy radiated on the discrete CPC ICSSWH entry aperture area over a time interval is obtained using equation 4.1,

$$Q_{incident} = I_{ave} A_{ap} \Delta t \tag{4.1}$$

where $Q_{incident}$ is the total amount of incident solar energy radiated on the discrete CPC ICSSWH entry aperture area (J), I_{ave} is the average global solar irradiance (W/m^2), A_{ap} is the area of the entry aperture (m^2) and Δt is the time interval (s). The entry aperture area is 0.354m^2.

The thermal energy collected by the discrete CPC ICSSWH is obtained using equation 4.2,

$$Q_{col} = m c_{water} (T_{f,\,heating} - T_{i,\,heating}) \tag{4.2}$$

where Q_{col} is the collected thermal energy (J), m is the mass of water (kg), c_{water} is the specific heat capacity of water (4184 J/kg·°C), $T_{f,\,heating}$ is the final heating temperature of the water (°C) and $T_{i,\,heating}$ is the initial heating temperature of the water (°C). The mass of the water is 17.67kg.

Based on the specification of discrete CPC ICSSWH as shown in Table 4.1 and the measurement results as depicted in Figures 4.1, the system efficiency of the discrete CPC ICSSWH, η_{sys} is attained for an interval of time Δt of an hour using equation 4.3, then the graph of system efficiency against the $\Delta T/I_{ave}$ where ΔT can be obtained using equation 4.4,

$$\eta_{sys} = \frac{mc_{water}(T_{f,\,heating} - T_{i,\,heating})}{I_{ave}A_{ap}\Delta t} \tag{4.3}$$

$$\Delta T = T_{ave,\,heating} - T_{ave,\,amb} \tag{4.4}$$

where the average water temperature in the storage tank over the period of heating for an interval time, Δt and the average ambient temperature over an interval time, Δt can be obtained using equation 4.5 and equation 4.6 respectively,

$$T_{ave,\,heating} = \frac{(T_{i,\,heating} + T_{f,\,heating})}{2} \tag{4.5}$$

$$T_{ave,\,amb} = \frac{(T_{i,\,amb} + T_{f,\,amb})}{2} \tag{4.6}$$

where $T_{i,heating}$ is the initial water temperature in the storage tank for the period of heating over the interval of time, Δt, $T_{f,heating}$ is the final water temperature in the storage tank for the period of heating over the interval of time, Δt, $T_{i,amb}$ is the initial ambient temperature over the interval of time, Δt and $T_{f,amb}$ is the final ambient temperature over the interval of time, Δt. Figure 4.2 displays the system efficiency of the discrete CPC ICSSWH.

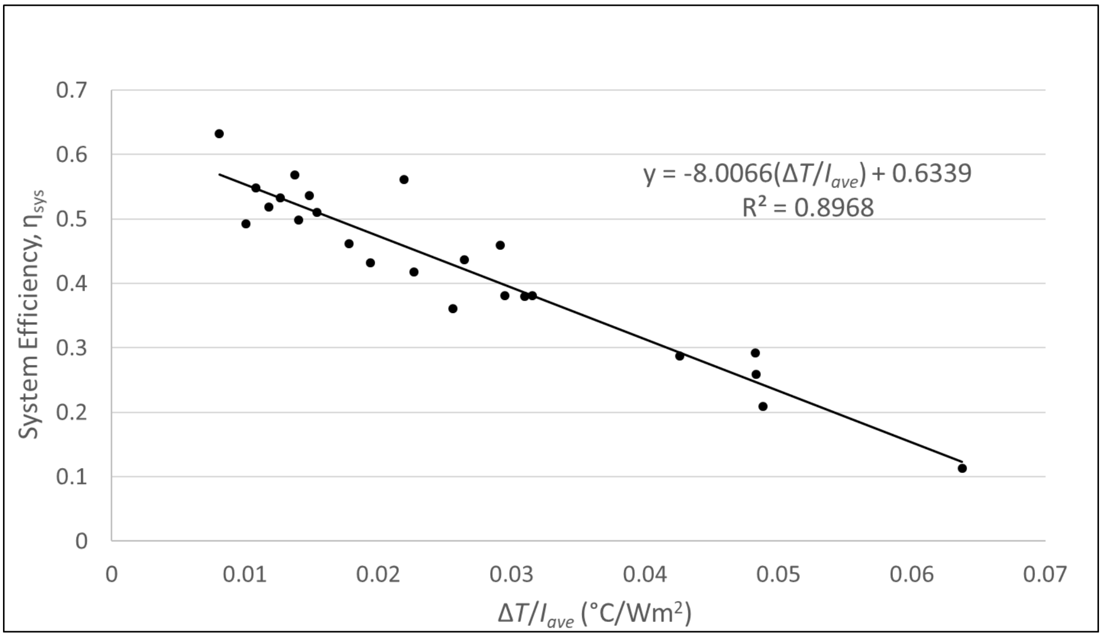

Figure 4.2: System Efficiency of the Discrete CPC ICSSWH

Based on Figure 4.2, the theoretical maximum system efficiency is 63.39% where the characterisation line intersects the system efficiency axis. The theoretical maximum water temperature achievable is 107.17°C assuming that the average global horizontal irradiance, I_{ave} is 1000W/m^2 constantly and the ambient temperature is 28°C.

4.2 Economic Analysis

The breakdown cost of all the components required for the construction of discrete CPC ICSSWH is tabulated. The major components required for the discrete CPC ICSSWH are piping system, solar collector and storage tank. The detailed components were summarised in Table 4.2.

Table 4.2: The Breakdown Cost for the Construction of the Discrete CPC ICSSWH

Component	Description	Quantity	Unit Price (RM)	Retail Price (RM)
Piping System	½’’ VIP full bore ball valve (340)	2 units	11.50/unit	23.00
	½’’ G.I. elbow	1 unit	1.40/unit	1.40
	½’’ K.C. nipple	2 units	1.80/unit	3.60
	½’’ steam nipple	1 unit	2.60/unit	2.60
	8’’ × ½’’ G.I. Pipe	2 units	6.90/unit	13.80
	Seal tape	2 units	0.60/unit	1.20
Solar Collector	2 units of construction adhesive sealant	2 units	8.48/unit	16.96
	1unit of 1124 mm × 492 mm × 5 mm clear float glass	1 unit	42.40/unit	42.40
	1144640 mm^2 of Mirror	1144640mm^2	$6.6 \times 10^{-5}/mm^2$	75.55
	3 units of Polyfoam	3 units	2.50/unit	7.50
	Plywood	2748680mm^2	$2.07 \times 10^{-5}/mm^2$	56.90
	Screw (25pieces/packet)	2 packets	1.80/packet	3.60
	Sealant silicone	2 units	7.10/unit	14.20
	Shellac	2 units	13.78/unit	27.56

Solar Collector (cont.)	Single sided signage 531 mm × 492 mm material 3mm transparency acrylic sheet	2 units	66.00/unit	132.00
	1’’ × 2’’ × 980 mm timber strip	6 units	2.383/unit	14.30
Storage Tank	Black paint	2 units	5.90/unit	11.80
	150mm (6’’) G.I. pipe	1m	122.192/m	122.19
	200 mm × 190mm × 5mm metal plate	2 units	20.00/unit	40.00
			Total Retail Cost (RM)	**610.56**

The payback period of the discrete CPC ICSSWH can be obtained using equation 4.7,

$$n_{pay} = -\frac{\ln(1 - S_{total} i' / P_{ann})}{\ln(1 + i')} \tag{4.7}$$

where *i’* can be obtained using equation 4.8,

$$i' = \left(\frac{1+i}{1+j}\right) - 1 \tag{4.8}$$

where S_{total} is the total retail cost of the discrete CPC ICSSWH (RM), P_{ann} is the annual saved fuel cost (RM/year), i is the interest rate and j is the inflation rate of the fuel.

A few considerations are made to calculate the payback period. If a loan is borrowed to construct the discrete CPC ICSSWH that can store 17.67 litres of hot water, the interest rate incurred is 3% and the inflation rate of the fuel is 4%. The daily heat energy required to increase the temperature of water from 25°C to 70.6°C is 0.9365 kWh. Hence, the annual energy saved is 341.809 kWh/year. The annual fuel cost saved is RM94.34/year provided the electricity cost is RM0.276/kWh. Therefore, the total payback period for the discrete CPC ICSSWH is 6.25 years if the borrowed loan is paid from the annual cost saved from the electricity bill.

CHAPTER 5

CONCLUSION AND RECOMMENDATIONS

In this study, a novel discrete CPC ICSSWH is proposed. The CPC collector is formed with several facet mirrors and then it was integrated to the ICSSWH system. A total of 5 mirrors are required to form the discrete CPC collector. The benefits of the discrete CPC ICSSWH are easy to be constructed and it is a passive system where sun tracking and active pump are not required. The performance of the discrete CPC ICSSWH are examined experimentally. From data collection, the discrete CPC ICSSWH has attained a maximum water temperature of 70.6°C. The theoretical maximum system efficiency of 63.39%. The discrete CPC ICSSWH can be fabricated easily and the total cost for the construction of the discrete CPC ICSSWH is RM610.56 and the payback period is 6.25 years.

There are some recommendations to improve the discrete CPC ICSSWH. In order to achieve better thermal insulation, double glazing can be fitted to the discrete CPC ICSSWH. Currently, the top side of the discrete CPC ICSSWH is covered with single clear float glass only. Hence, the installation of double glazing allows better heat retention, thus heat loss especially at night can be further minimised. Furthermore, better insulation material can be added in between the gap of the front covers and the supporting frame and also the gap between the solar collector and the discrete CPC ICSSWH side covers to further reduce the heat loss.

The second recommendation is to install another storage tank to collect the heated water. The mentioned storage tank must be fully insulated for optimum thermal insulation. The current discrete CPC ICSSWH is meant for domestic us only. The heat losses in the discrete CPC ICSSWH will increase at higher temperature. Therefore, when the water reaches the desired temperature for domestic uses, it can be draw off to the fully insulated storage tank so that the heated water can be retained for a longer period of time. Furthermore, the heated water must be drawn off completely to the fully insulated tank at night to reduce the heat loss to the surrounding at a faster pace.

The third recommendation is change the storage tank with higher thermal conductivity. This is to ensure that solar energy radiated on it can be absorbed at better efficiency and the water can be heated at a faster rate. For instance, copper tank or brass tank can be incorporated to the discrete CPC ICSSWH to heat up the water at a shorter time.

REFERENCES

Alghoul, M.A., Sulaiman, M.Y., Azmi, B.Z. and Wahab, M. A., 2005. Review of materials for solar thermal collectors. *Anti-Corrosion Methods and Materials*, 52 (4), pp. 199-206.

Close, D.J., 1962. The performance of solar water heaters with natural convection. *Solar Energy*, 6(1), pp. 33-40.

Devanarayanan, K. and Murugavel, K.K., 2014. Integrated collector storage solar water heater with compound parabolic concentrator – development and progress. *Renewable and Sustainable Energy Reviews*, 39, pp. 51-64.

Duffie, J.A. and Beckham, W.A., 2013. *Solar Engineering of Thermal Processes*. 4th ed. New Jersey: John Wiley & Sons, Inc.

Goswami, D.Y., 2015. *Principles of Solar Engineering*. 3rd ed. Boca Raton: Taylor & Francis Group.

Jayakanth, J. J., Ramasubramanian, S., Chandrasekaran, M. and Manavalan, S., 2017. Investigation of solar water heater by using flat plate collector and evacuated tubes. *International Conference on Emerging Trends in Engineering Research*.

Kumar, R. and Rosen, M. A., 2011. Integrated collector-storage solar water heater with extended storage unit. *Applied Thermal Engineering*, 31, pp. 348-354.

Kumar, R. and Rosen, M. A., 2010. Thermal performance of integrated collector storage solar water heater with corrugated absorber surface. *Applied Thermal Engineering*, 30, pp. 1764-1768.

Makofske, W.J., 2015. Renewing with Renewables: Direct Solar Energy Use in Developing Countries. *Disaster by Design: The Aral Sea and its Lessons for Sustainability*, 20, pp. 357-371.

Martínez-Rodríguez, G., Fuentes-Silva, A.L. and Picón-Núñez, M., 2017. Solar thermal networks operating with evacuated-tube collectors. Energy, pp. 1-8.

Morley, T., 2017. *Advantages and Disadvantages of Solar Water Heating Panels*. [online] Available at: <http://www.greenpower-technology.co.uk/news-and-advice/advantages-and-disadvantages-of-solar-water-heating-panels/> [Accessed 1 July 2017].

Ramlow, B. and Nusz, B., 2010. *Solar water heating: a comprehensive guide to solar water and space heating systems*. [e-book] Canada: New Society Publishers. Available through: Google Books <books.google.com> [Accessed 1 July 2017].

Sabiha, M.A., Saidur, R., Mekhilef, S. and Mahian, O., 2015. Progress and latest developments of evacuated tube solar collectors. *Renewable and Sustainable Energy Reviews*, 51, pp. 1038-1054.

Singh, R., Lazarus, I.J. and Souliotis, M., 2015. Recent developments in integrated collector storage (ICS) solar water heaters: A review. *Renewable and Sustainable Energy Reviews*, 54, pp. 270-298.

Singh, S. K., Singh, A. K., Yadav, S. K., 2012. Design and Fabrication of Parabolic Trough Solar Water Heater for Hot Water Generation. *International Journal of Engineering Research & Technology (IJERT)*, 1(10), pp. 1–9.

Souliotis, M., Chemisana, D., Caouris, Y.G. and Tripanagnostopoulos, Y., 2012. Experimental study of integrated collector storage solar water heaters. *Renewable Energy,* 50, pp. 1083-1094.

Twidell, J. and Weir, T., 2015. *Renewable Energy Resources*. 3rd ed. New York: Routledge.

Varghese, J., Samsher and Manjunath, K., 2016. A parametric study of a concentrating integral storage solar water heater for domestic uses. *Applied Thermal Engineering*, 111, pp. 734-744.

APPENDICES

APPENDIX A: Data Collection

Date: 25th January 2018

Time	GHI	T_1	T_2	T_3	Time	GHI	T_1	T_2	T_3	Time	GHI	T_1	T_2	T_3
0900					1200	721 708 726 761 773	36.9	40.6	30.6	1500	996 847 952 756 567	50.5	54.9	35.0
0905					1205	747 736 705 705 692	37.2	41.0	31.4	1505	525 474 591 533 538	50.7	54.9	34.6
0910					1210	702 699 646 667 712	37.8	41.9	31.4	1510	472 452 603 879 900	50.8	54.8	34.3
0915					1215	720 699 695 677 647	38.3	42.6	31.2	1515	570 452 524 456 421	51.0	55.1	34.2
0920					1220	630 633 636 631 611	38.7	43.0	31.0	1520	419 601 702 789 727	51.4	55.2	33.5
0925					1225	599	39.2	43.4	31.5	1525	666	51.7	55.8	34.2

						600					480			
						619					311			
						640					289			
						645					270			
						606					214			
						595					285			
0930					1230	588	39.5	43.9	31.8	1530	200	51.9	55.2	33.6
						601					194			
						657					148			
						641					137			
						650					136			
0935					1235	617	40.1	44.3	32.1	1535	123	51.9	55.0	32.2
						584					129			
						585					129			
						597					126			
						590					123			
0940					1240	609	40.6	44.9	32.0	1540	127	52.0	54.6	32.6
						607					138			
						608					155			
						598					164			
						576								
0945					1245	559	41.5	45.5	32.4	1545		51.9	54.1	32.2
						534								
						553								
						575								
						585								
0950					1250	588	41.5	45.8	31.7	1550				
						590								
						578								
						576								
						566								
0955					1255	563	41.8	46.0	31.6	1555				
						556								
						550								
						532								
						535								
1000					1300	529	42.5	46.8	31.3	1600				
						525								
						511								
						506								
						507								
1005					1305	500	42.7	46.8	31.8	1605				
						471								
						438								
1010	318	30.1	32.7	26.7	1310	421	43.3	47.1	32.1	1610				

	320					433								
	315					435								
	321					444								
	286					445								
	276					451								
	258					447								
1015	272	30.4	32.7	26.8	1315	427	43.4	47.2	31.0	1615				
	272					439								
	289					426								
	297					404								
	297					438								
1020	299	30.5	32.9	27.0	1320	440	43.9	47.6	31.9	1620				
	291					446								
	276					449								
	290					447								
	308					438								
1025	298	30.6	33.2	27.3	1325	441	44.1	47.7	32.0	1625				
	310					433								
	327					443								
	339					460								
	349					462								
1030	359	30.8	33.5	27.8	1330	453	44.4	47.9	31.8	1630				
	374					447								
	382					456								
	371					453								
	367					480								
1035	368	31.1	33.8	28.0	1335	488	44.8	48.3	32.0	1635				
	360					470								
	343					478								
	337					482								
	346					497								
1040	347	31.4	34.1	28.5	1340	493	45.1	48.8	32.0	1640				
	345					502								
	348					515								
	344					507								
	353					506								
1045	358	31.7	34.4	27.5	1345	491	45.3	49.0	32.4	1645				
	363					507								
	365					526								
	377					561								
	382					562								
1050	386	31.9	34.7	28.0	1350	579	45.7	49.4	32.1	1650				
	387					597								
	375					613								
1055	356	32.2	34.9	28.1	1355	617	46.0	49.6	32.1	1655				

	362					613								
	360					585								
	355					557								
	361					531								
1100	374	32.5	35.3	28.3	1400	497	46.5	49.9	32.5	1700				
	407					466								
	386					467								
	404					480								
	432					482								
1105	453	32.7	35.6	27.9	1405	485	46.6	50.0	32.0					
	462					530								
	499					542								
	508					550								
	529					627								
1110	548	33.0	36.0	28.0	1410	623	47.0	50.6	32.2					
	541					660								
	535					652								
	554					650								
	521					670								
1115	494	33.4	36.6	28.7	1415	671	47.3	51.2	33.2					
	518					682								
	527					689								
	526					722								
	463					714								
1120	462	33.6	36.9	28.8	1420	725	47.6	51.8	32.8					
	433					731								
	422					680								
	403					660								
	383					623								
1125	377	34.0	37.1	29.1	1425	639	48.3	52.4	33.0					
	374					674								
	346					644								
	324					532								
	322					506								
1130	324	34.3	37.4	28.8	1430	463	48.3	52.3	33.5					
	332					481								
	340					514								
	523					377								
	576					352								
1135	573	34.6	37.7	28.9	1435	358	48.7	52.1	32.9					
	591					475								
	595					491								
	573					487								
	560					466								
1140	566	34.9	38.2	29.3	1440	450	49.2	52.4	33.3					

	579 582 590 600					421 419 434 360								
1145	595 591 610 630 640	35.4	38.8	29.8	1445	378 413 460 530 501	49.2	52.5	32.9					
1150	609 592 657 671 658	35.7	39.1	29.5	1450	479 703 727 917 863	49.3	52.6	33.9					
1155	637 669 683 651 682	36.2	39.7	30.2	1455	956 748 831 934 913	49.8	53.9	33.6					

Date: 10th February 2018

Time	GHI	T_1	T_2	T_3	Time	GHI	T_1	T_2	T_3	Time	GHI	T_1	T_2	T_3
0900	82 97 98 85 86	31.0	31.1	24.6	1200	774 780 790 796 792	44.5	49.4	33.0	1500	228 221 236 258 249	60.5	64.2	37.0
0905	88 89 90 92 92	31.1	31.3	24.9	1205	804 777 767 780 781	45.5	50.4	33.4	1505	239 233 232 265 265	60.3	63.8	35.2
0910	93 95 96 97 101	31.1	31.2	25.2	1210	798 794 799 811 819	45.6	50.3	34.5	1510	278 308 353 430 636	60.4	63.5	34.4
0915	114 112 105 105 106	31.1	31.3	25.3	1215	818 815 782 790 728	46.7	51.7	34.4	1515	645 615 627 660 628	60.3	63.6	37.0

	107					669					646			
	110					694					670			
0920	118	31.2	31.3	25.8	1220	715	46.9	51.9	34.5	1520	685	60.7	63.9	35.5
	180					741					664			
	263					758					626			
	316					753					682			
	333					748					715			
0925	334	31.2	31.5	25.7	1225	749	48.2	52.8	35.2	1525	694	61.0	64.6	37.0
	337					735					664			
	335					694					676			
	340					648					577			
	343					557					469			
0930	348	31.2	31.5	26.0	1230	524	48.6	53.1	35.2	1530	443	61.4	64.9	36.0
	353					436					425			
	357					365					412			
	362					346					418			
	366					330					423			
0935	370	31.3	32.0	26.8	1235	319	48.9	53.5	34.6	1535	459	61.6	64.6	37.2
	372					326					488			
	374					362					603			
	378					375					610			
	385					411					715			
0940	387	31.5	32.6	26.6	1240	513	49.3	53.6	34.6	1540	680	61.8	64.7	37.0
	408					598					626			
	400					519					580			
	415					542					504			
	408					428					489			
0945	412	31.5	32.8	26.2	1245	653	49.3	52.9	33.6	1545	495	62.2	65.0	37.0
	413					688					522			
	419					650					548			
	421					600					549			
	424					682					638			
0950	431	31.6	33.1	26.6	1250	881	49.7	53.0	34.9	1550	615	62.5	65.1	36.3
	440					861					630			
	442					640					678			
	445					485					768			
	451					592					627			
0955	453	31.9	33.8	27.7	1255	456	49.9	54.0	33.9	1555	608	62.5	65.2	36.9
	456					438					510			
	456					390					498			
	458					415					519			
	463					465								
1000	468	32.4	34.5	27.5	1300	445	50.7	54.9	34.1	1600		62.8	65.5	36.5
	471					426								
	475					435								

1005	477	32.6	34.5	28.3	1305	415	51.3	54.9	34.2	1605				
	477					437								
	480					467								
	484					523								
	485					678								
1010	484	33.1	35.6	27.4	1310	745	51.6	55.3	34.6	1610				
	488					676								
	493					880								
	493					1122								
	500					670								
1015	504	33.2	35.6	28.5	1315	669	51.9	55.9	34.6	1615				
	511					673								
	515					595								
	521					556								
	524					550								
1020	527	34.0	36.8	29.2	1320	554	52.6	56.7	35.2	1620				
	532					556								
	535					553								
	539					565								
	540					561								
1025	547	34.0	37.0	29.0	1325	548	52.6	56.9	35.0	1625				
	542					604								
	543					597								
	545					620								
	550					632								
1030	556	34.9	38.5	29.3	1330	681	52.9	57.0	34.3	1630				
	564					715								
	566					800								
	568					787								
	571					777								
1035	574	34.9	38.6	30.6	1335	803	53.6	57.8	36.5	1635				
	575					720								
	576					694								
	580					666								
	583					742								
1040	587	35.3	38.8	29.7	1340	615	54.0	58.1	35.9	1640				
	595					664								
	602					663								
	607					683								
	611					702								
1045	611	36.2	40.1	29.6	1345	766	54.7	59.0	36.3	1645				
	614					696								
	618					661								
	620					663								
	620					702								

	635					712								
	644					732								
1050	652	36.3	40.1	31.4	1350	729	54.8	59.3	36.5	1650				
	660					701								
	664					683								
	661					623								
	664					684								
1055	668	36.7	40.4	29.1	1355	674	55.3	59.8	35.6	1655				
	672					664								
	670					665								
	674					641								
	678					655								
1100	678	37.7	41.7	30.5	1400	684	55.8	60.0	34.8	1700				
	685					683								
	686					710								
	689					707								
	692					659								
1105	691	37.8	41.8	31.2	1405	709	56.2	60.5	36.3					
	699					719								
	699					716								
	705					695								
	710					695								
1110	720	38.9	43.3	31.3	1410	708	56.7	60.5	36.2					
	717					724								
	721					800								
	723					852								
	727					850								
1115	728	38.9	43.3	31.3	1415	875	57.0	61.0	36.0					
	733					950								
	738					896								
	738					989								
	743					890								
1120	748	39.9	43.9	31.4	1420	765	57.5	61.7	37.5					
	746					672								
	744					651								
	752					711								
	739					613								
1125	742	39.9	44.5	32.2	1425	602	58.0	61.8	37.2					
	741					556								
	751					531								
	756					471								
	757					388								
1130	757	41.4	45.9	32.1	1430	382	58.3	62.0	37.5					
	763					459								
	761					695								

	775					500								
	779					702								
1135	784	41.4	46.0	32.2	1435	746	58.4	62.5	37.1					
	795					769								
	791					448								
	793					791								
	793					954								
1140	732	41.9	47.0	32.5	1440	968	58.7	62.5	36.0					
	727					961								
	728					941								
	732					911								
	735					838								
1145	748	42.6	47.8	33.0	1445	849	58.9	62.7	36.3					
	745					831								
	749					877								
	753					857								
	757					851								
1150	761	42.8	48.0	33.4	1450	843	59.6	63.8	36.6					
	761					679								
	773					878								
	774					874								
	771					846								
1155	776	44.4	49.0	32.9	1455	833	60.3	64.7	36.3					
	775					297								
	774					243								

Date: 2nd March 2018

Time	GHI	T_1	T_2	T_3	Time	GHI	T_1	T_2	T_3	Time	GHI	T_1	T_2	T_3
						749					679			
						768					705			
0900					1200	773	41.3	45.6	32.0	1500	698	62.6	66.7	37.4
						782					692			
						783					717			
						774					731			
						774					707			
0905					1205	770	42.0	46.3	33.0	1505	661	63.0	67.0	36.2
						781					677			
						777					692			
						779					713			
0910					1210	789	42.5	46.9	31.6	1510	724	63.3	67.1	37.0
						788					698			
						790					754			

						800					710			
	164					805					652			
	176					822					632			
0915	181	31.4	32.2	26.9	1215	833	43.1	47.6	32.8	1515	647	63.6	67.3	37.2
	181					850					627			
	187					849					634			
	193					860					594			
	221					850					586			
0920	233	31.4	32.4	27.0	1220	855	43.7	48.3	32.7	1520	630	64.0	67.5	37.1
	230					852					580			
	236					850					618			
	240					860					656			
	248					860					688			
0925	243	31.6	32.6	27.2	1225	858	44.5	49.2	33.0	1525	700	64.3	67.8	36.3
	226					850					743			
	216					869					608			
	226					894					741			
	231					911					754			
0930	234	31.7	32.9	27.3	1230	909	45.3	50.2	33.5	1530	728	64.5	67.9	36.0
	251					918					739			
	260					905					796			
	288					889					817			
	276					927					773			
0935	278	31.9	33.0	27.7	1235	917	45.8	50.8	33.2	1535	752	64.8	68.1	36.8
	220					878					738			
	195					917					734			
	286					907					766			
	302					923					723			
0940	308	32.0	33.3	27.8	1240	919	46.5	51.5	34.0	1540	721	65.0	68.5	37.9
	293					961					725			
	292					974					715			
	290					960					715			
	287					974					689			
0945	297	32.2	33.6	27.8	1245	980	47.1	52.4	34.0	1545	704	65.5	68.9	36.6
	292					992					707			
	293					474					740			
	290					918					744			
	283					492					707			
0950	272	32.3	33.9	27.7	1250	982	48.0	53.0	33.9	1550	705	65.7	69.2	37.0
	268					990					704			
	261					1031					701			
	264					1035					697			
0955	270	32.5	34.0	28.0	1255	666	48.5	53.8	34.0	1555	719	66.0	69.6	37.5
	277					576					654			
	280					940					302			

	284					1003					282			
	280					1017					253			
	271					1016					250			
1000	270	32.7	34.3	27.9	1300	1014	49.1	54.4	34.9	1600	259	66.5	69.8	36.7
	274					993					606			
	283					433					703			
	281					289					676			
	283					278					731			
1005	287	32.9	34.5	28.4	1305	683	49.8	54.4	34.3	1605	757	66.3	69.6	35.3
	286					1054					743			
	287					1043					748			
	290					1044					741			
	290					1040					698			
1010	292	33.0	34.8	27.9	1310	1009	50.1	55.4	34.8	1610	702	66.5	69.9	37.2
	299					983					695			
	305					977					740			
	316					991					710			
	317					1007					329			
1015	319	33.3	35.0	28.2	1315	999	50.8	56.0	34.2	1615	740	66.9	70.2	36.6
	321					1001					720			
	325					995					734			
	324					993					719			
	324					994					702			
1020	324	33.5	35.3	28.7	1320	992	51.7	57.0	34.9	1620	670	67.1	70.4	37.5
	327					987					675			
	330					976					669			
	334					982					645			
	334					991					636			
1025	337	33.7	35.6	28.8	1325	984	52.2	57.6	35.6	1625	632	67.4	70.6	36.9
	335					991					630			
	338					999					631			
	345					1000					652			
	347					1012					654			
1030	353	33.9	35.9	28.8	1330	1011	52.8	58.2	34.9	1630	667	67.5	70.8	36.2
	352					1005					655			
	353					1005					623			
	359					1005					608			
	359					1005					638			
1035	366	34.3	36.3	29.0	1335	1004	53.7	59.2	35.9	1635	629	67.7	70.9	37.0
	369					1005					578			
	370					1006					606			
	373					993					604			
1040	380	34.4	36.6	29.2	1340	997	54.4	60.0	35.6	1640	595	67.9	71.1	37.5
	379					992					606			
	377					980					576			

	380					987					605			
1045	378	34.6	36.8	29.6	1345	991	54.9	60.5	35.9	1645	607	68.0	71.1	37.1
	393					999					627			
	403					1003					614			
	403					997					613			
	404					988					620			
1050	408	35.0	37.3	29.7	1350	992	55.5	61.1	36.5	1650	641	68.1	71.2	37.2
	420					994					603			
	421					1004					604			
	420					1009					594			
	421					1001					617			
1055	425	35.3	37.8	29.6	1355	991	56.3	61.9	37.1	1655	600	68.5	71.7	37.4
	426					995					618			
	425					1005					618			
	436					1006					604			
	448					994					624			
1100	451	35.6	38.2	29.5	1400	997	56.6	62.1	36.9	1700	628	68.6	71.7	37.4
	463					973								
	466					1013								
	475					1003								
	485					1009								
1105	500	35.9	38.6	29.5	1405	1012	57.2	62.5	37.5					
	494					995								
	496					1001								
	501					1016								
	503					990								
1110	536	36.4	39.2	29.7	1410	946	57.7	63.0	38.0					
	558					942								
	570					938								
	579					987								
	592					1003								
1115	594	36.8	39.9	30.5	1415	1008	58.2	63.3	36.2					
	590					997								
	598					995								
	597					996								
	603					995								
1120	607	37.2	40.6	30.2	1420	1000	58.7	63.8	37.5					
	616					1012								
	608					1012								
	621					1007								
	636					990								
1125	643	37.7	41.1	30.5	1425	995	59.3	64.3	37.5					
	654					1009								
	657					1018								
	661					1019								

	676					1005								
1130	672	38.0	41.7	31.0	1430	1024	59.9	64.9	36.8					
	668					1009								
	669					1008								
	677					942								
	676					905								
1135	674	38.6	42.6	31.8	1435	891	60.5	65.3	36.4					
	681					875								
	700					839								
	701					830								
	707					847								
1140	706	39.4	43.1	31.7	1440	827	61.1	65.9	37.3					
	699					827								
	701					811								
	701					753								
	707					765								
1145	720	39.8	43.7	31.6	1445	742	61.5	66.2	38.4					
	717					745								
	719					735								
	723					751								
	724					716								
1150	721	40.5	44.5	32.4	1450	682	61.9	66.4	36.8					
	720					685								
	722					681								
	721					696								
	719					710								
1155	723	40.8	44.9	32.1	1455	755	62.3	66.6	36.5					
	728					702								
	725					698								
	735					682								
	741					695								

Date: 17th March 2018

Time	GHI	T_1	T_2	T_3	Time	GHI	T_1	T_2	T_3	Time	GHI	T_1	T_2	T_3
0900					1200	883	45.7	49.8	34.2	1500	947	68.0	72.1	38.6
						883					934			
						884					943			
						878					934			
						881					975			
0905					1205	887	46.4	50.5	35.1	1505	994	68.4	72.6	38.6
						887					982			
						881					783			

						888					402			
						896					455			
						890					974			
						903					956			
0910					1210	918	47.5	51.4	35.8	1510	933	68.8	72.6	37.5
						907					927			
						912					706			
						918					299			
						921					335			
0915					1215	922	48.0	52.1	35.9	1515	844	69.3	72.7	36.1
						930					941			
						889					653			
	108					901					805			
	80					917					957			
0920	195	29.3	29.5	25.9	1220	925	48.6	52.5	34.1	1520	913	69.6	73.2	37.0
	189					930					894			
	134					928					990			
	101					930					873			
	100					933					701			
0925	99	29.3	29.7	28.1	1225	934	49.2	53.3	35.9	1525	323	70.2	73.9	37.2
	98					944					311			
	101					930					305			
	102					931					299			
	118					933					305			
0930	165	29.5	29.9	26.8	1230	947	49.7	54.0	36.8	1530	308	70.3	73.5	37.9
	174					959					346			
	167					955					527			
	138					950					815			
	109					940					874			
0935	130	29.5	29.9	26.0	1235	950	50.5	54.6	34.5	1535	862	70.3	73.6	37.4
	132					965					340			
	169					959					324			
	172					955					326			
	164					978					331			
0940	202	29.6	31.2	28.3	1240	986	51.1	55.3	35.6	1540	355	70.5	73.4	36.2
	250					993					534			
	217					997					723			
	128					998					641			
	131					991					490			
0945	139	29.8	31.3	28.6	1245	988	51.8	55.9	34.6	1545	610	70.5	73.5	38.1
	128					990					418			
	117					998					273			
	123					994					237			
0950	133	30.0	32.1	27.8	1250	1000	52.3	56.4	35.9	1550	228	70.6	73.1	36.0
	184					1009					248			

	351					1005					283			
	475					1011					316			
	369					1016					484			
	259					1017					455			
0955	293	30.1	32.1	27.5	1255	1015	53.0	57.0	35.4	1555	473	70.4	72.9	35.0
	269					1005					450			
	351					1005					516			
	471					1004					565			
	492					1008					550			
1000	544	30.4	32.5	28.7	1300	1020	53.7	57.7	35.0	1600	620	70.4	73.0	37.3
	583					1019					608			
	586					1023					472			
	586					1027					395			
	591					1018								
1005	593	30.7	33.8	28.8	1305	991	54.4	58.4	36.5	1605		70.6	73.0	37.6
	595					984								
	600					983								
	604					981								
	604					994								
1010	607	31.2	34.5	29.9	1310	990	55.1	59.0	34.3	1610				
	613					993								
	616					985								
	620					987								
	626					999								
1015	629	31.8	35.2	30.8	1315	1003	55.8	59.8	35.5	1615				
	619					1014								
	633					1030								
	634					1030								
	644					1028								
1020	644	32.2	35.8	29.8	1320	987	56.4	60.5	36.0	1620				
	644					990								
	648					1037								
	652					1020								
	655					1015								
1025	647	32.7	36.5	32.9	1325	1001	57.1	61.1	36.0	1625				
	652					1006								
	655					1012								
	662					1004								
	667					990								
1030	670	33.3	37.1	32.5	1330	996	57.8	61.7	35.5	1630				
	674					994								
	675					987								
	680					991								
1035	680	33.8	37.7	29.9	1335	994	58.5	62.2	38.0	1635				
	687					1005								

	691					1002								
	692					1001								
1040	697	34.5	38.3	33.2	1340	994	59.0	62.9	36.5	1640				
	702					991								
	707					990								
	710					988								
	713					993								
1045	713	35.1	38.9	33.2	1345	994	59.6	63.5	36.9	1645				
	720					995								
	722					1003								
	724					1001								
	729					1003								
1050	730	35.8	39.6	30.5	1350	996	60.2	64.1	36.0	1650				
	733					1007								
	736					1018								
	738					1015								
	742					1027								
1055	743	36.5	40.2	31.8	1355	1018	60.8	64.8	37.7	1655				
	743					1008								
	748					1002								
	749					1006								
	751					1005								
1100	755	36.9	40.7	31.4	1400	1003	61.4	65.4	38.9	1700				
	762					1010								
	763					1011								
	764					1012								
	767					1011								
1105	771	37.6	41.3	31.6	1405	996	62.0	66.1	36.5					
	774					1008								
	779					1031								
	784					1035								
	788					1034								
1110	787	38.3	42.2	32.5	1410	1035	62.5	66.5	38.3					
	789					1044								
	790					1040								
	792					905								
	796					838								
1115	799	39.2	43.3	32.5	1415	727	62.9	66.7	36.3					
	792					998								
	796					1003								
	796					1015								
	802					1019								
1120	802	40.1	44.0	30.8	1420	1021	63.6	67.8	38.7					
	809					1013								
	817					1005								

	823					997								
	827					977								
	829					967								
	832					978								
1125	834	40.7	44.6	33.5	1425	987	64.2	68.3	38.2					
	833					993								
	832					993								
	830					997								
	829					1004								
1130	834	41.3	45.3	32.2	1430	995	64.7	68.8	40.8					
	843					987								
	845					985								
	846					975								
	843					950								
1135	843	42.1	46.0	32.7	1435	965	65.4	69.5	37.2					
	845					968								
	848					965								
	851					960								
	856					966								
1140	857	42.9	46.7	33.2	1440	968	65.9	70.0	39.5					
	861					978								
	861					966								
	863					955								
	863					968								
1145	870	43.6	47.5	35.2	1445	968	66.5	70.6	38.6					
	876					962								
	891					978								
	886					993								
	883					997								
1150	877	44.3	48.2	33.9	1450	972	66.9	71.0	37.5					
	876					958								
	877					945								
	874					936								
	876					934								
1155	873	45.0	49.1	33.7	1455	930	67.4	71.5	38.1					
	878					925								
	886					947								